

# Multiplicity distributions in $pp/p\bar{p}$ and $e^+e^-$ collisions with parton recombination

I. Zborovský\*

*Nuclear Physics Institute,  
Academy of Sciences of the Czech Republic,  
Řež, Czech Republic*

A new approach to phenomenological description of the charged particle multiplicity distributions in  $pp/p\bar{p}$  and  $e^+e^-$  collisions is presented. The observed features of the data are interpreted on the basis of stochastic-physical ideas of multiple production. Besides the processes of parton immigration and absorption, two and three parton incremental and decremental recombinations are considered. The complex behaviour of the multiplicity distributions at different energies is described by four parametric generalized hypergeometric distribution (GHD). Application of the proposed GHD to data measured by the CMS, ALICE, and ATLAS Collaborations suggests that soft multiparton recombination processes can manifest itself significantly in the structure of multiplicity distribution in  $pp$  interactions at very high energies.

PACS numbers: 13.85.Hd, 13.66.Bc

Keywords: multiplicity distribution, high energy, parton recombination, cascade processes

## I. INTRODUCTION

The multiple production of particles in high energy collisions received a lot of attention during many years. A renewal interest in this topic originated recently with the beginning of operation of the Large Hadron Collider (LHC) at CERN. Among first results obtained at the LHC were multiplicity measurements in proton-proton collisions. The CMS, ALICE, and ATLAS Collaborations provided valuable and precise data on multiplicity distributions (MD) of the charged hadrons in the new super high energy domain. The study of multiparticle production can give important information about parton processes and transitions of the colored partons to the colorless hadrons. The complex phenomena that influence MD are however very hard to describe in detail, because we cannot formulate the multiparton process in terms of its QCD theory. Most of the particles which contribute to the multiplicity buildup are soft particles and a perturbative approximation is inapplicable here. Second, hadronization should be somehow taken into account which is far of being understood properly. The natural and probably most economical approach is to look for empirical relations and regularities.

The study of particle production as a function of multiplicity has revealed a very popular Koba-Nielsen-Olesen (KNO) scaling [1]. In  $pp/p\bar{p}$  collisions, the scaling in the full phase-space holds up to the highest energy of the CERN Intersecting Storage Rings (ISR) but it is clearly violated [2] in the energy region of the CERN Super Proton Synchrotron (SPS) collider and beyond. The strong violation of KNO scaling was observed also at the energy  $\sqrt{s} = 7$  TeV in the limited pseudorapidity intervals ( $|\eta| < 2.4$ ) though for small pseudorapidity windows ( $|\eta| < 0.5$ ) the scaling is approximately valid [3]. A related phenomenon is the so-called negative binomial regularity, which is the occurrence of the negative binomial distribution (NBD) in different interactions over a wide range of the collision energies. The UA5 Collaboration showed that MD in the non-single-diffractive (NSD)  $pp/p\bar{p}$  collisions can be described by NBD up to the energy  $\sqrt{s} = 546$  GeV both in the full phase-space [4] and in symmetric pseudorapidity windows [5]. Analysis of data on MD measured by the ALICE Collaboration indicates [6, 7] that NBD describes the data in the small pseudorapidity window  $|\eta| < 0.5$  up to the energy  $\sqrt{s} = 2360$  GeV. Besides  $pp/p\bar{p}$  collisions, NBD has been applied to various systems including  $e^+e^-$  annihilations. Much effort has been made to explain the negative binomial form of MD observed in many situations, however, its physical origin has not been fully understood [8].

The shape of MD of particles produced in hadron-hadron collisions at high energies is quite different. The full phase-space data on charged particle multiplicities obtained from the NSD events in  $p\bar{p}$  collisions at  $\sqrt{s} = 900$  GeV [9] indicated that besides KNO, the negative binomial regularity is violated as well. The measurements of MD at the energy  $\sqrt{s} = 1800$  GeV by the E735 Collaboration [10] at the Fermilab Tevatron showed even stronger deviation of data from NBD. Though with large mutual discrepancies at high multiplicities, both data demonstrate a narrow peak at the maximum and some structure around  $n \sim 2 < n >$ . Despite its correct qualitative behaviour, the single NBD is not sufficient to describe the experimental data. A systematic study of the complex form of MD was performed

---

\* Electronic address: zborovsky@ujf.cas.cz

in the framework of two component model [11] and its three component modification [12]. There exist also other approaches to explanation of the observed features of particle production at high energies (for a review see Ref. [8]). New interest in this field is motivated by the recent results of the multiplicity measurements in  $pp$  collisions at the LHC. The data obtained by the CMS [3], ALICE [13], and ATLAS [14] Collaborations show similar structure in MD of charged particles produced in the limited windows in pseudorapidity. The measurements allow to study evolution of the distinct peak at maximum and the broad shoulder at large  $n$  both with the collision energy and pseudorapidity.

In this paper we propose an alternative phenomenological approach to the description of MD in  $pp/p\bar{p}$  and  $e^+e^-$  collisions. Using the same concept for hadron and lepton interactions, we try to account for the structure in data which emerges in the  $pp/p\bar{p}$  interactions at high energies. The proposed four parametric representation of MD is motivated by a scenario of the parton cascading. The considerations behind are based on a premise that dynamics of the particle production as manifested on the level of multiplicities can be described in terms of a stochastic cascading with specific types of the underlying processes. The construction includes the processes of parton immigration and absorption together with two and three parton incremental and decremental recombination. The recombination processes are assumed in the final stage of the parton evolution during the color neutralization. The transition to the colorless hadrons is considered in a stationary regime at breakdown of the confinement and onset of hadronization.

## II. RECURRENCE RELATION BETWEEN MULTIPLICITIES $N$ AND $N+1$

The number of particles created in high energy collisions varies from event to event. The distributions of probabilities  $P_n$  of occurrence of the multiplicity  $n$  provide sensitive means to probe dynamics of the interaction. Besides general characteristics of particle production the distributions contain information about multiparticle correlations in an integrated form. The correlations of the final particles reflect features of hadronization mechanism and properties of the QCD parton evolution just before hadronization. The data on MD of charged particles from the high energy  $pp/p\bar{p}$  and  $e^+e^-$  interactions allow us to study the processes underlying the multiple production and its correlation structure within a phenomenological framework of parton cascading. The extraction of information on these processes requires the elementary charge conservation to be taken into account. In our approach we investigate and exploit MD of charged particle pairs and characterize it by a recurrence relation between  $P_n$  and  $P_{n+1}$ . This assumes connection between the collisions of multiplicities  $n+1$  with  $n+1$  collisions of multiplicity  $n$  which can be written in the form

$$\frac{(n+1)P_{n+1}}{P_n} = g(n). \quad (1)$$

The class of MD defined by expression of this type has been considered with a view to stimulated emission and cascading in Ref. [15]. The independent emission of particles represented by Poisson distribution is characterized by  $g(n) = c$ . The constancy of  $g(n)$  means that creation of an additional particle is independent of number of other particles. The stimulated emission of identical bosons obeying Bose-Einstein statistics follows geometric distribution for which one has  $g(n) = c(n+1)$ . This means that emission probability of a boson is enhanced by a factor  $n+1$  when  $n$  bosons are already present in the system. Both examples are special cases of NBD given by the formula

$$P_n = \frac{(n+k-1)!}{n!(k-1)!} q^n (1-q)^k. \quad (2)$$

The distribution depends on two parameters  $q = \langle n \rangle / (\langle n \rangle + k)$  and  $k$  for which the recurrence relation (1) is given by the linear dependence

$$g(n) = (k+n)q. \quad (3)$$

For fixed  $\langle n \rangle$ , the Poisson distribution is recovered with  $q, k^{-1} \rightarrow 0$ . The geometric distribution corresponds to  $k = 1$ . Chew et al. proposed [16] a generalization of NBD which gives good description of MD of charged particles in  $e^+e^-$  annihilation [17]. The generalized multiplicity distribution (GMD) has the form

$$P_n = \frac{(n+k-1)!}{(n-k')!(k-1)!} q^{n-k'} (1-q)^{k+k'}. \quad (4)$$

The distribution is function of three parameters  $q = (\langle n \rangle - k') / (\langle n \rangle + k)$ ,  $k$ , and  $k'$ . The expression for  $g(n)$  in this case reads

$$g(n) = \frac{(n+1)(k+n)}{(n+1-k')} q. \quad (5)$$

The formula for GMD reduces to the expression for NBD, when  $k' = 0$ . For  $k = 0$ , GMD becomes Furry-Yule distribution (FYD) proposed by Hwa and Lam [18]. The mentioned distributions are fully determined by the functional form of  $g(n)$  together with the general normalization condition to unity. The normalization is guaranteed for  $n > k' - 1$  by the linear dependence of  $g(n)$  at large multiplicities with  $q < 1$ . In the parton cascade picture of multiple production the parameters of these distributions can be related with the rate constants of branching processes in the evolution equations for probabilities.

### A. Cascade processes with parton recombination

In a high energy collision with the creation of a multiparticle state the dynamics of the system can be simulated as a parton cascading associated with quark and gluon interactions during the interaction time. The corresponding parton cascade processes inspired by the elementary perturbative QCD are of three types: a/ parton-parton collisions, b/ branching processes such as quark bremsstrahlung, gluon self interaction or gluon splitting, c/ fusion processes e.g. gluon annihilation on a quark. Practically all QCD-based models of many-body production involve some form of cascading. The stochastico-physical picture of the multiplicity evolution can be described by Kolmogorov-Chapman differential-difference (DD) rate equations [19] for the probability  $P_n(t)$ . The continuous parameter  $t$  is usually interpreted as an ordering parameter, QCD evolution parameter, or time. The rate equations were applied to hadron physics many years ago in Ref. [20]. Soon afterwards, the properties of MD were studied by solving DD equations in terms of parton cascading by number of people [21]. In particular, all possible QCD vertices were taken into account in Ref. [22]. Stationary regime in birth and death processes with recombination (confluence) of two ( $2 \rightarrow 1$ ) and three ( $3 \rightarrow 1$ ) gluons has been investigated in Ref. [23].

In this paper we point out and exploit somewhat different strategy. We try to establish minimal number of such processes in the cascade picture of particle production which could account for both the general character of MD and its complex structure observed at high energies. A successful description of experimental data requires essential features of the cascade evolution to be introduced into the phenomenology. We attempt to estimate those features which mostly influence the building structure of MD at high energies. This involves processes of parton recombinations at the end of the cascade just near breakdown of the confinement. The last phase of the parton evolution is considered to have large impact on the form of MD of the produced hadrons. We suppose that in the final stage there exists some kind of a stationary regime which occurs at the transition between parton and hadron degrees of freedom. In this regime, soft partons intensively exchange their momenta to reach an "momenta uniformity" before their conversion into observable particles [23].

In order to introduce features of parton recombination into a multiplicity description, we consider a stationary regime of DD equations of Kolmogorov-Chapman type. Hereafter we refer to the partons as objects which cascade in "time" and regard the terms particle and parton as interchangeable. The binary parton-parton scatterings do not change the number of particles during the system evolution but can influence neutralization or screening of the color flow. They can act as supporting processes which initiate branching or fusion of the nearby partons. Such connection represents multiparton interactions contributing to a change of the particle number by one. The simplest interactions of this type are recombinations of two or three particles. Here we consider the process of two parton incremental recombination ( $2 \rightarrow 3$ ) together with three parton incremental ( $3 \rightarrow 4$ ) and three parton decremental ( $3 \rightarrow 2$ ) recombination processes. The confluence of two and three partons,  $2 \rightarrow 1$  and  $3 \rightarrow 1$ , is supposed to be negligible with respect to other recombination processes at the end of the cascade. Together with the particle production that depends on particles already produced, we consider independent immigration ( $0 \rightarrow 1$ ) and absorption ( $1 \rightarrow 0$ ) as another source of partons influenced by bulk properties of the system created in the collision. The accumulated energy is transformed into partons in this manner, or on the contrary a parton can be melted and absorbed by the expanding system again. In the case of independence of each cascade process, the corresponding DD evolution equations for the probability  $P_n(t)$  read

$$\begin{aligned} \dot{P}_n = & + \alpha_0 P_{n-1} - \alpha_0 P_n \\ & + \beta_0 (n+1) P_{n+1} - \beta_0 n P_n \\ & + \alpha_2 (n-1)(n-2) P_{n-1} - \alpha_2 n(n-1) P_n \\ & + \alpha_3 (n-1)(n-2)(n-3) P_{n-1} - \alpha_3 n(n-1)(n-2) P_n \\ & + \beta_2 (n+1)n(n-1) P_{n+1} - \beta_2 n(n-1)(n-2) P_n. \end{aligned} \quad (6)$$

The coefficients  $\alpha_0, \alpha_2, \alpha_3$  are the corresponding rates for the processes  $0 \rightarrow 1, 2 \rightarrow 3, 3 \rightarrow 4$ , respectively. Similar parameters for degradation of the particle number in the processes  $1 \rightarrow 0$  and  $3 \rightarrow 2$  are denoted as  $\beta_0$  and  $\beta_2$ . Using

the definition of the generating function

$$Q(w) = \sum_{n=0}^{\infty} P_n w^n, \quad (7)$$

we rewrite the system of DD equations (6) in terms of  $Q(w)$ . The corresponding stationary solution ( $\dot{P}_n = 0$ ) satisfies the third order differential equation

$$\alpha_0 Q(w) - \beta_0 \frac{dQ(w)}{dw} + \alpha_2 w^2 \frac{d^2 Q(w)}{dw^2} + (\alpha_3 w^3 - \beta_2 w^2) \frac{d^3 Q(w)}{dw^3} = 0. \quad (8)$$

A regular solution of this equation is proportional to the generalized hypergeometric function

$$Q(w) = {}_3F_2 \left( a_1, a_2, a_3; b_1, b_2, \frac{\alpha_3}{\beta_2} w \right) \quad (9)$$

The complex constants  $a_i$  and  $b_j$  are given in terms of the real parameters  $\alpha_0$ ,  $\alpha_2$ ,  $\alpha_3$ ,  $\beta_0$ , and  $\beta_2$  (see Appendix A). The ratio (1) is given as follows

$$\frac{(n+1)P_{n+1}}{P_n} = \frac{\alpha_0 + \alpha_2 n(n-1) + \alpha_3 n(n-1)(n-2)}{\beta_0 + \beta_2 n(n-1)}. \quad (10)$$

This recurrence relation together with the normalization condition for  $P_n$  fully determines the formula for MD which we refer to as the generalized hypergeometric distribution (GHD). The distribution depends on four parameters  $\alpha_0/\beta_2$ ,  $\alpha_2/\beta_2$ ,  $\alpha_3/\beta_2$ , and  $\beta_0/\beta_2$  which are ratios of the rate constants for the corresponding cascade processes.

In the next section we exploit GHD to describe MD of the charged particles produced in  $pp/p\bar{p}$  and  $e^+e^-$  interactions. The formula (10) has various limits applicable for both reactions at different energies and phase space regions. If  $\alpha_0 \rightarrow 0$  and  $\beta_0 \rightarrow 0$  simultaneously, GHD reduces to NBD. In that case  $g(n)$  is given by (3) with the parameters  $q = \alpha_3/\beta_2$  and  $k = \alpha_2/\alpha_3 - 2$ . On the contrary, if  $\alpha_0$  and  $\beta_0$  are both large enough relative to other parameters, a Poisson-like peak appears in MD at small  $n$  for which  $g(n) \simeq \alpha_0/\beta_0$ . There exists a region where GHD can be narrower than Poisson distribution. This happens at low energies where the rate constants  $\alpha_2$  and  $\alpha_3$  are small or even vanish.

### III. ANALYSIS OF DATA

The statistics of the charged particle MD is governed by the requirements of conservation laws in each collision. Due to the global charge conservation, there are only even multiplicities when dealing with experimental data in the full phase-space. On the other hand the charge conservation cannot be satisfied by the stochastic processes which are independent of the charge. In particular, GHD, as defined for all non-negative integer values of  $n$ , cannot directly represent the full phase-space data on multiplicities which are always even. There are two main conceptions how to tackle the problem. According to the often used procedure [4], the probabilities for only even integers  $n$  are taken from a theoretical distribution, then are renormalized and compared to the measured values of  $P_n$ . The second approach assumes to deal with MD of particle pairs and compare it to a theoretical distribution for all values of  $n$ . Both methods give different values of the parameters entering the distribution and differ also in capability of description of experimental data. Here we use the second method and apply GHD and NBD (for comparison) to the distribution of particle pairs.

We have analysed experimental data on MD of charged particles produced in the non-single-diffractive (NSD)  $pp/p\bar{p}$  collisions in the full phase-space. The analysis was performed with the high energy data measured by the E735 Collaboration [10] at  $\sqrt{s} = 1800, 1000, 546$ , and 300 GeV, by the UA5 Collaboration [24] at  $\sqrt{s} = 900$  and 200 GeV, and by the ABCDHW Collaboration [25] at  $\sqrt{s} = 63, 53, 45$ , and 30 GeV. The study includes also the FNAL fixed target data [26–29] at  $\sqrt{s} = 27.6, 23.8, 19.7$ , and 13.8 GeV corrected for diffraction cross sections [30], the Serpukhov data at  $\sqrt{s} = 11.5$  GeV [31] with diffraction corrections [32] and the low energy CERN data [33] measured by the BHM Collaboration at  $\sqrt{s} = 6.8$  and 4.9 GeV. The results of the analysis with the CERN-MINUIT program are shown in Table I and in Figs. 1-2. As can be seen from Table I, the description of MD of particle pairs by NBD is in most cases unsatisfactory including the data from ISR and lower energies. Though MD of the charged particles can be approximated by NBD up to the energy  $\sqrt{s} = 200$  GeV pretty well, NBD is not able to account fully for the narrower distribution of the particle pairs. At the energies lower than  $\sqrt{s} \sim 20$  GeV, the distribution becomes even narrower than Poisson distribution. This corresponds to negative values of the parameters  $k$  and  $q$ , meaning that NBD

TABLE I: The results of analysis of MD of the charged particle pairs in the NSD  $pp/p\bar{p}$  collisions in the full phase-space.

$\sqrt{s}$ (GeV)		NBD			GHD				
		k	q	$\chi^2/\text{NDF}$	$\alpha_0/\beta_2$	$\alpha_2/\beta_2$	$\alpha_3/\beta_2$	$\beta_0/\beta_2$	$\chi^2/\text{NDF}$
1800	E735	$3.36 \pm 0.04$	$0.877 \pm 0.001$	670/126	$(2.7 \pm 0.4)10^3$	$17 \pm 1$	$0.76 \pm 0.01$	$341 \pm 41$	30.1/124
1000	E735	$3.4 \pm 0.1$	$0.854 \pm 0.003$	106/75	$(5.0 \pm 2.1)10^3$	$27 \pm 8$	$0.57 \pm 0.09$	$600 \pm 234$	54.5/73
900	UA5	$4.0 \pm 0.1$	$0.815 \pm 0.005$	84.4/52	$(1.2 \pm 0.9)10^3$	$64 \pm 2$	-	$1545 \pm 94$	11.0/51
546	E735	$5.0 \pm 0.1$	$0.776 \pm 0.002$	165/78	$(2.5 \pm 1.2)10^3$	$19 \pm 6$	$0.61 \pm 0.08$	$339 \pm 155$	29.8/76
300	E735	$5.4 \pm 0.2$	$0.776 \pm 0.005$	52/58	$(1.1 \pm 1.0)10^3$	$16 \pm 7$	$0.49 \pm 0.14$	$193 \pm 154$	14.3/56
200	UA5	$5.8 \pm 0.3$	$0.64 \pm 0.01$	13.3/29	$(3.6 \pm 0.7)10^2$	$33 \pm 3$	-	$573 \pm 96$	3.2/28
63	ISR	$21 \pm 2$	$0.25 \pm 0.02$	30.1/18	$1.7 \pm 4.3$	$5.3 \pm 0.2$	$0.29 \pm 0.03$	$0.2 \pm 0.5$	19.8/16
53	ISR	$24 \pm 3$	$0.21 \pm 0.02$	30/19	$16 \pm 15$	$4.6 \pm 2.3$	$0.34 \pm 0.04$	$2.2 \pm 2.3$	4.6/17
45	ISR	$59 \pm 20$	$0.09 \pm 0.03$	44.9/17	$15 \pm 9$	$4.1 \pm 0.4$	$0.36 \pm 0.06$	$1.5 \pm 1.1$	4.5/15
30	ISR	$49 \pm 21$	$0.10 \pm 0.04$	22.5/15	$0.5 \pm 2.0$	$4.5 \pm 0.3$	$0.16 \pm 0.05$	$0.03 \pm 0.13$	4.5/13
27.6	FNAL	$36 \pm 17$	$0.11 \pm 0.05$	22.1/14	$5 \pm 10$	$3.8 \pm 0.5$	$0.22 \pm 0.08$	$0.6 \pm 1.6$	15.5/12
23.8	FNAL	$(19 \pm 3)10^4$	$(24 \pm 4)10^{-6}$	12.2/12	$6 \pm 10$	$4.0 \pm 0.4$	$0.07 \pm 0.07$	$0.8 \pm 1.8$	7.6/10
19.7	FNAL	$(-8 \pm 5)10^3$	$(-5 \pm 3)10^{-4}$	24/11	$3.6 \pm 3.6$	$3.8 \pm 0.4$	$0.00 \pm 0.07$	$3.6 \pm 3.6$	4.5/9
13.8	FNAL	$-13 \pm 1$	$-0.35 \pm 0.04$	46.5/8	$4.6 \pm 1.2$	$2.8 \pm 0.1$	-	$0.5 \pm 0.2$	8.0/7
11.5	Serpukhov	$-14 \pm 1$	$-0.28 \pm 0.03$	23.7/7	$4.7 \pm 2.0$	$2.3 \pm 0.1$	-	$0.8 \pm 0.5$	8.8/6
6.8	CERN/BHM	$-5.0 \pm 0.2$	$-0.90 \pm 0.10$	4.7/3	$7.9 \pm 5.0$	$0.5 \pm 0.4$	-	$1.3 \pm 1.3$	0.2/2
4.9	CERN/BHM	$-4.1 \pm 0.1$	$-0.64 \pm 0.03$	25.5/3	$3.5 \pm 0.3$	-	-	$0.9 \pm 0.2$	5.4/3

transforms to a binomial one. By virtue of its four parameters, GHD describes the complex structure of the charged particle MD emerging in the high energy  $pp/p\bar{p}$  collisions in the full phase-space sufficiently well. This is illustrated in Fig.1(a) on data [10] from the E735 Collaboration where a peak at low  $n$  and a shoulder at large multiplicities is visible. The evolution of the observed structure with the energy  $\sqrt{s}$  is shown in more detail in Fig.1(b). Here the relative residues of MD with respect to the NBD parametrization are depicted. The residues are mutually shifted by factors 2 for single energies. The lines correspond to the description of data with GHD. As one can see from Fig.1(b), the shoulder broadens with the energy  $\sqrt{s}$  and its maximum moves towards larger multiplicities. This corresponds to an increase of the parameter  $\alpha_3/\beta_2$  which is ratio of the rate constants for the processes  $3 \rightarrow 4$  and  $3 \rightarrow 2$ . The measurements of MD by the UA5 collaboration at  $\sqrt{s} = 200$  and 900 GeV in the full phase-space lay systematically below the E735 data [10] for large  $n$ . The discrepancy has a consequence that the parameter  $\alpha_3/\beta_2$  is negative for the UA5 data. Therefore we set it to null in our analysis in this particular case (see Table I).

The description of data on MD by GHD in the NSD proton-proton collisions at the ISR energies is shown in Fig.2(a). The relative residues with respect to the NBD parametrizations are depicted in Fig.2(b). The residues are mutually shifted by factor 2 for single energies. One can see from Fig.2(b) that NBD does not represent accurate parametrization of MD of particle pairs even at the ISR energies. Especially for low  $n$  the residues of data relative to NBD show remnants of the peaky structure which is clearly visible in the TeV energy region. The solid lines represent the parametrization of data by GHD. The small experimental errors allow good determination of  $\alpha_2/\beta_2$  and  $\alpha_3/\beta_2$  in this region. The values of the parameters are non-zero at the ISR energies but they are smaller than at the TeV energies. Similarly, the parameters  $\alpha_0/\beta_2$  and  $\beta_0/\beta_2$  are non-zero though both are relatively small. This is once again a reformulation of the statement that NBD is not sufficient to describe MD of the particle pairs nevertheless at the ISR energies it provides much better approximation of data than in the TeV energy region.

The analysis of MD below  $\sqrt{s} \sim 20$  GeV showed that the parameter  $\alpha_3$  becomes negative. Therefore we set it equal to null in this region. It means that the process  $3 \rightarrow 4$  dies out as the first at low energies. For still smaller  $\sqrt{s}$  there is not enough energy even for the process  $2 \rightarrow 3$  and GHD becomes two parameter distribution. In this region, MD of particle pairs is extremely narrow. The non-zero value of  $\beta_2$  makes it narrower than the Piosson distribution. This means that the parton recombination process  $3 \rightarrow 2$  remains active till the very small energies though it brings along only the diminution of the particle number.

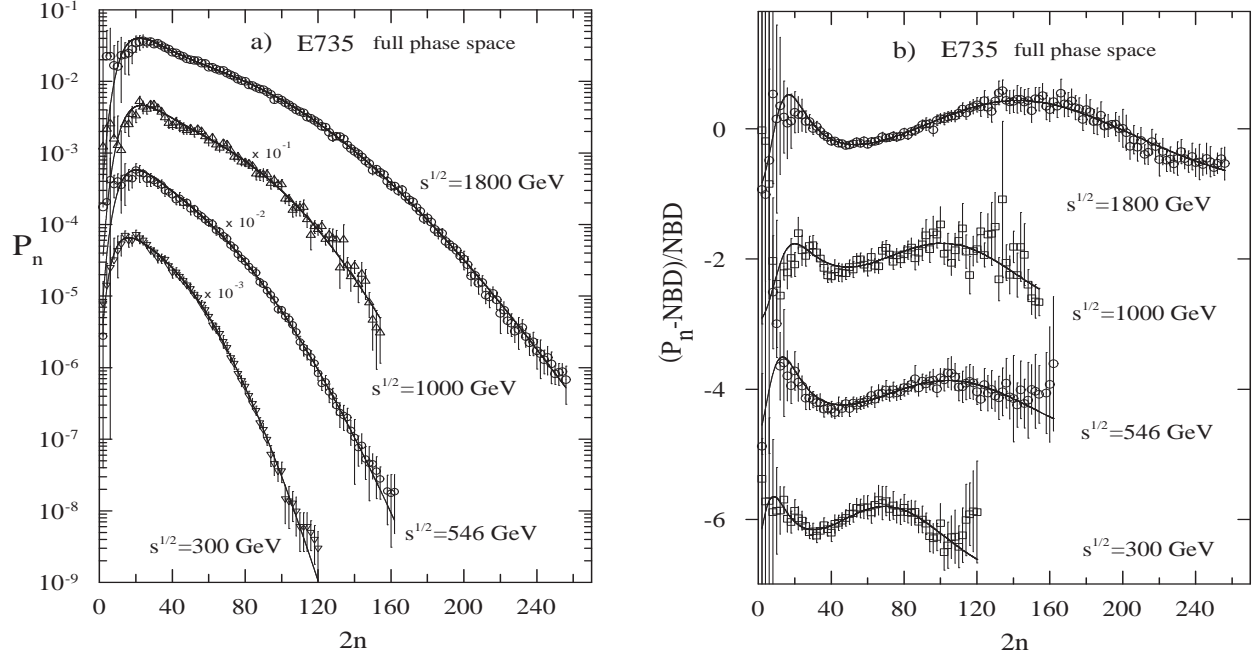


FIG. 1: (a) MD of charged particles in the NSD  $p\bar{p}$  collisions at energies  $\sqrt{s} = 300 - 1800$  GeV. The data [10] are multiplied by the indicated factors. (b) The relative residues of MD with respect to the NBD parametrization. The residues are mutually shifted by the factor of 2 at different energies. The lines represent description of the data by GHD.

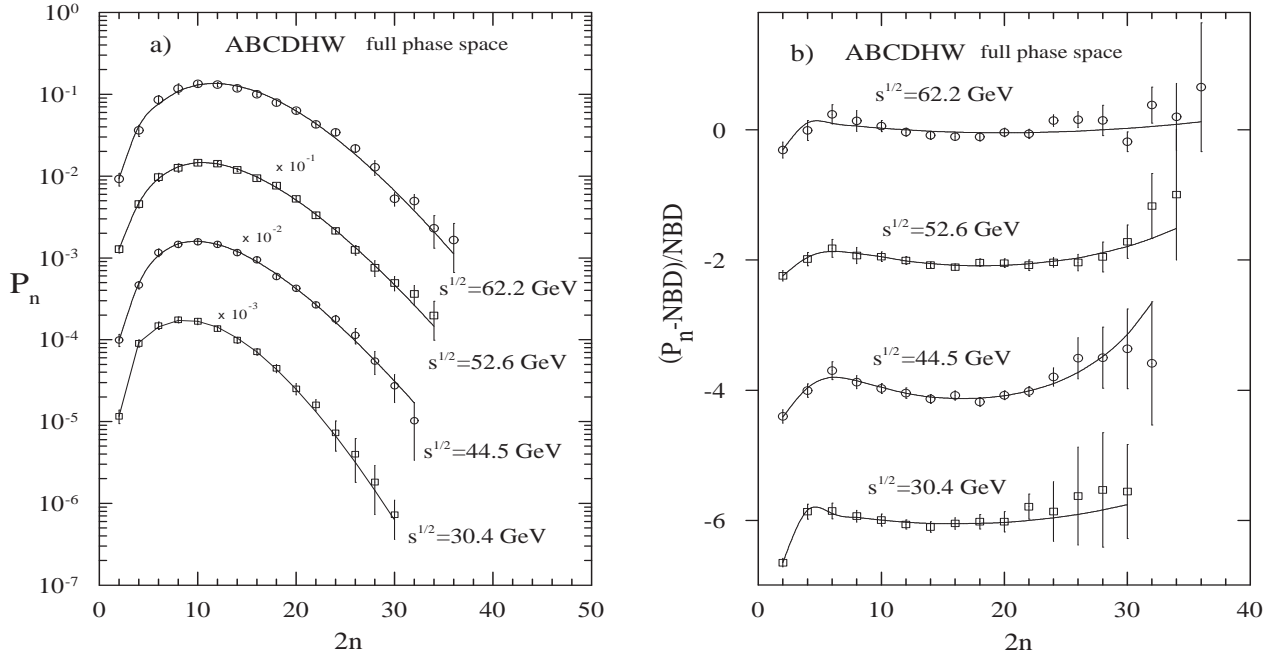


FIG. 2: (a) MD of charged particles in the NSD  $pp$  collisions at the ISR energies. The data [25] are multiplied by the indicated factors. (b) The relative residues of MD with respect to the NBD parametrization. The residues are mutually shifted by the factor of 2 at different energies. The lines represent description of the data by GHD.

### A. Structure of multiplicity in limited phase-space regions

Recently, the CMS Collaboration provided results of systematic measurements of charged particle multiplicities in  $pp$  collisions at the LHC. The data [3] were accumulated in five pseudorapidity ranges from  $|\eta| < 0.5$  to  $|\eta| < 2.4$  at the collision energies  $\sqrt{s} = 900, 2360$ , and  $7000$  GeV. The measurements of MD in the restricted phase-space regions can serve as a sensitive probe of the underlying dynamics in various phenomenological models.

For an adequate description one needs to make additional assumptions when projecting the full phase-space data onto the smaller pseudorapidity windows  $|\eta| < \eta_c$ . The odd-even effect of the charged particle distribution  $P_n^{ch}$  is smeared out with the decreasing  $\eta_c$  and the distribution fills all values of  $n$ . We avoid the complication concerning the charged particle measurements in the limited phase-space regions and collect the data in the neighbouring even and odd bins as follows

$$P_n = P_{2n}^{ch} + P_{2n-1}^{ch}, \quad n = 1, 2, \dots, \quad (11)$$

so simulating the distribution of particle pairs. It would be more correct to deal with MD of negative particles which is essentially the distribution of the charged particle pairs. Nevertheless, application of GHD to the distribution (11) allows us to establish main trends which characterize MD of negative particles. Here we study the dependence of the parameters  $\alpha_0/\beta_2$ ,  $\alpha_2/\beta_2$ ,  $\alpha_3/\beta_2$ , and  $\beta_0/\beta_2$  on the size of the pseudorapidity span  $|\eta| < \eta_c$ .

In Fig. 3(a) we show MD of charged particles in the limited phase-space regions measured by the CMS Collaboration in  $pp$  collisions at  $\sqrt{s} = 7000$  GeV. The CMS data for the five pseudorapidity ranges from  $|\eta| < 0.5$  to  $|\eta| < 2.4$  are collected in the neighbouring even and odd bins in multiplicity (11) and multiplied by the powers of 0.2 for different  $\eta_c$ . The data confirm existence of the complex structure observed in MD by the E735 and UA5 Collaborations at energies  $\sqrt{s} = 900$ - $1800$  GeV in the full phase-space. At  $\sqrt{s} = 7000$  GeV, the peaky form at low  $n$  and a shoulder at high multiplicities is seen in the all five measured  $\eta_c$ -windows. The peak becomes most prominent and the shoulder most wide for  $|\eta| < 2.4$ . The evolution of the structure with  $\eta_c$  is demonstrated in Fig. 3(b) in more detail where the relative residues of the data with respect to the NBD parametrization are depicted. For the sake of clarity the residues are mutually shifted by unity for different pseudorapidity intervals. The solid lines represent a description of the data by GHD. One can see from Fig.3(b) that at the energy  $\sqrt{s} = 7000$  GeV the residual structure survives even down to  $\eta_c = 0.5$ . As a consequence, NBD is not sufficient to describe the data well enough neither for small pseudorapidity windows at this super high energy.

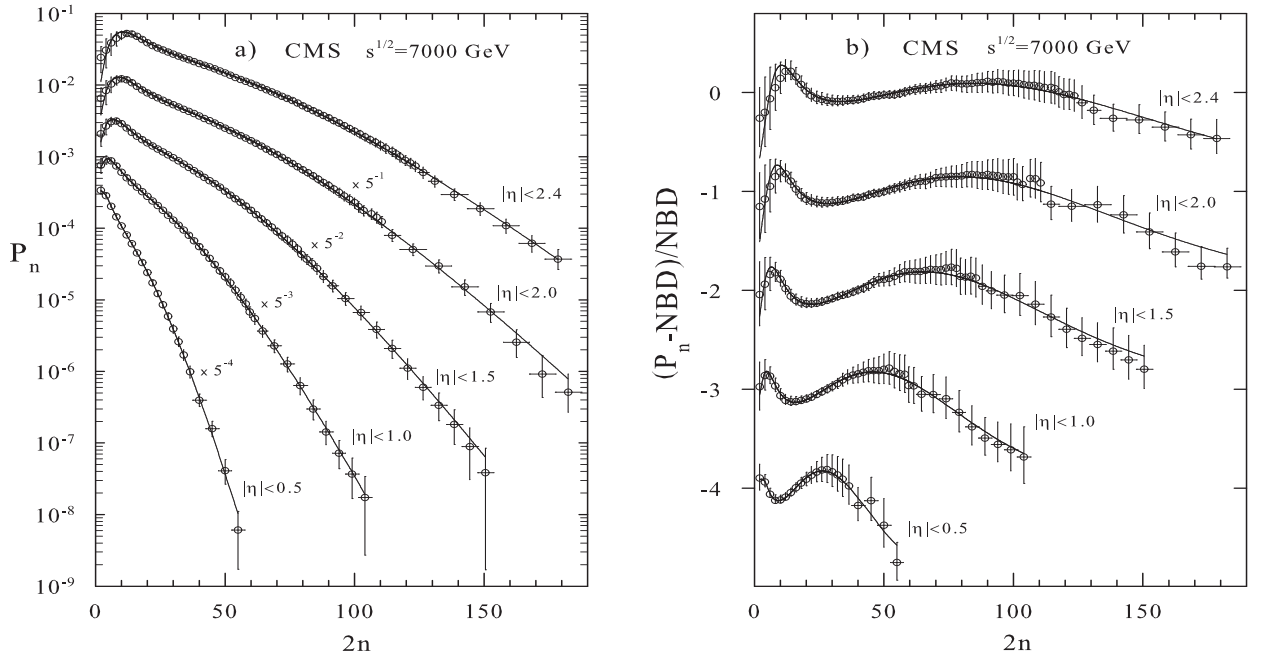


FIG. 3: (a) MD of charged particles in the limited phase-space regions from the NSD  $pp$  collisions at  $\sqrt{s} = 7000$  GeV. The data [3] are accumulated in the neighbouring even and odd bins and multiplied by the indicated factors. (b) The corresponding relative residues with respect to the NBD parametrization. The residues are shifted mutually by unity for different  $\eta_c$ . The lines represent description of the data with GHD.

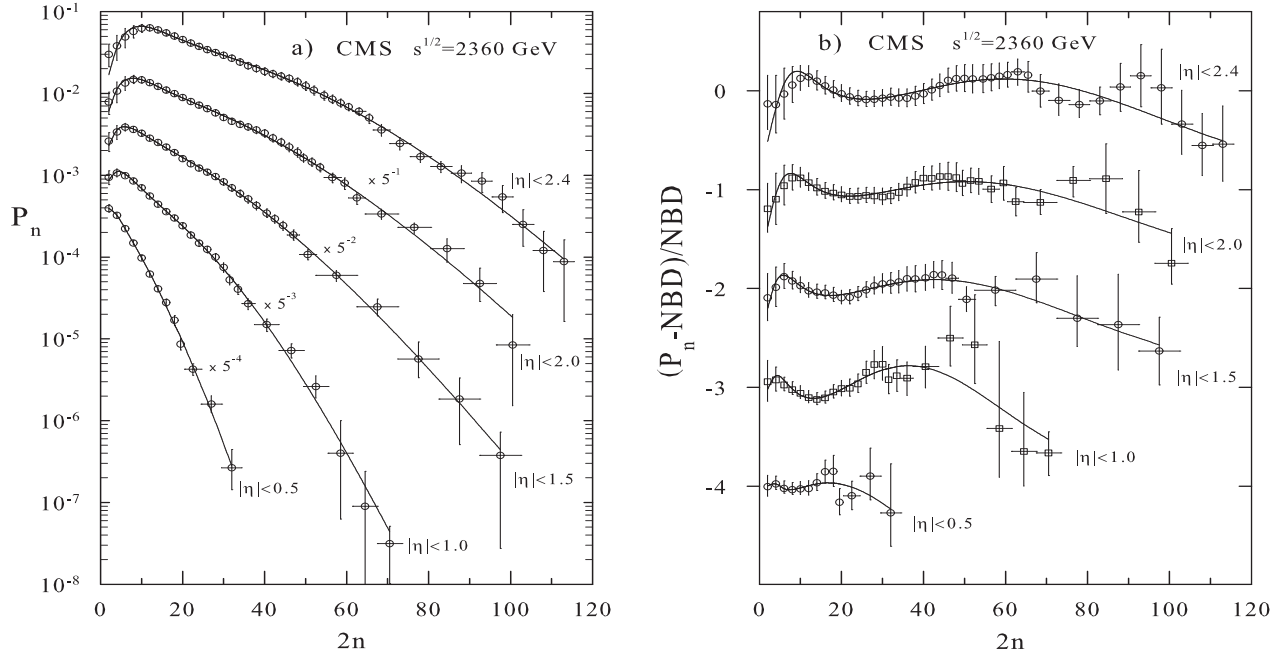


FIG. 4: (a) MD of charged particles in the limited phase-space regions from the NSD  $pp$  collisions at  $\sqrt{s} = 2360$  GeV. The data [3] are accumulated in the neighbouring even and odd bins and multiplied by the indicated factors. (b) The corresponding relative residues with respect to the NBD parametrization. The residues are shifted by unity for different  $\eta_c$ . The lines represent description of the data with GHD.

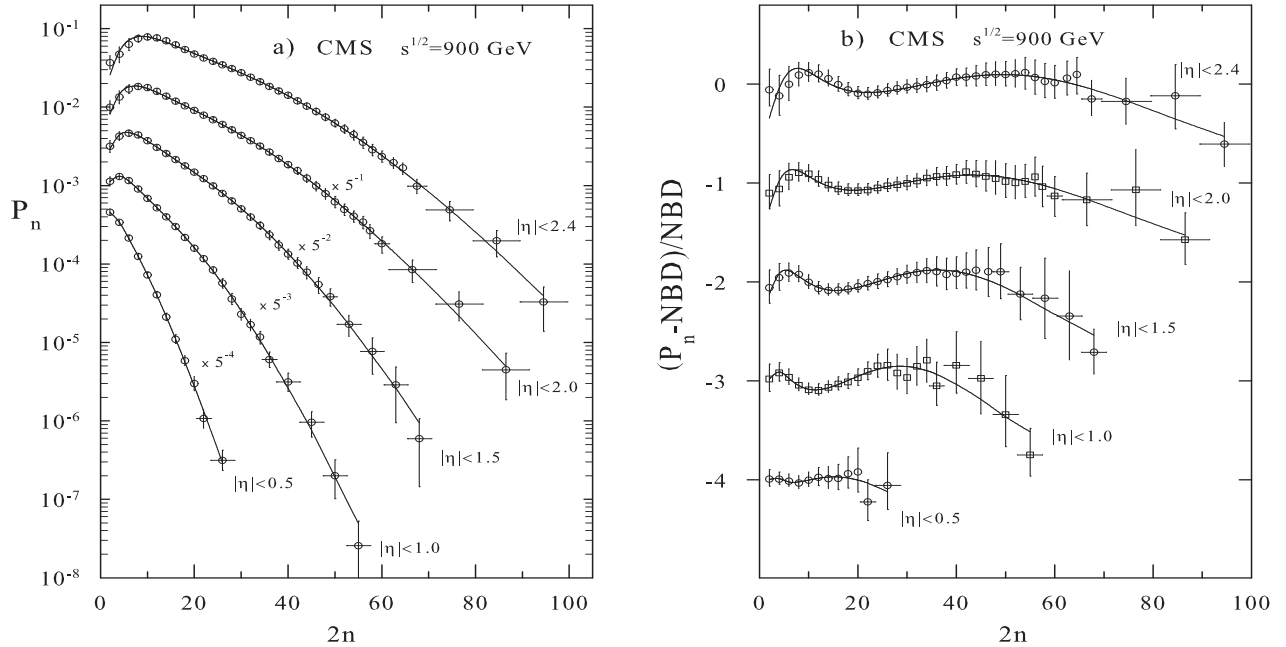


FIG. 5: (a) MD of charged particles in the limited phase-space regions from the NSD  $pp$  collisions at  $\sqrt{s} = 900$  GeV. The data [3] are accumulated in the neighbouring even and odd bins and multiplied by the indicated factors. (b) The corresponding relative residues with respect to the NBD parametrization. The residues are shifted by unity for different  $\eta_c$ . The lines represent description of the data with GHD.



The CMS data measured at the energies  $\sqrt{s} = 2360$  GeV and  $\sqrt{s} = 900$  GeV are presented in the same fashion in Fig. 4 and Fig. 5, respectively. A similar structure as in Fig. 3 is visible also at these energies. The systematic measurements of the CMS Collaboration allow us to study the evolution of the observed structure with  $\sqrt{s}$ . One can see from Figs. 3(b), 4(b), and 5(b) that the peak at low  $n$  becomes more distinct with the increasing energy.

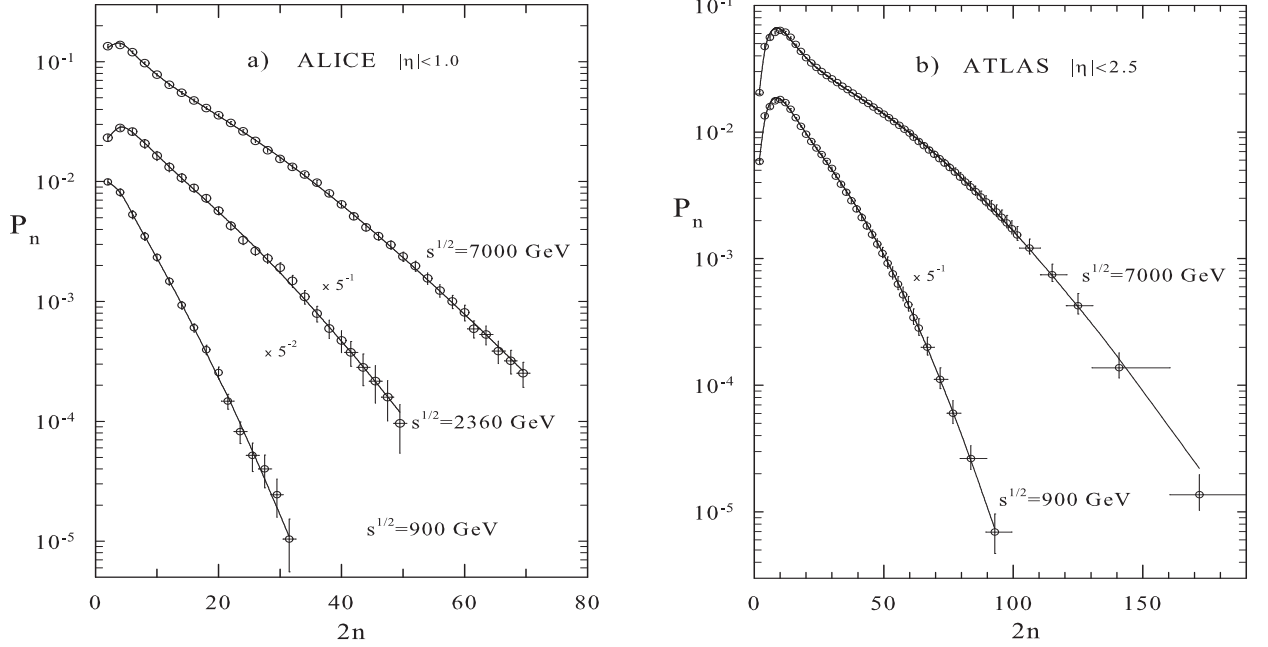


FIG. 6: (a) MD of charged particles obtained by the ALICE Collaboration [13] at the energies  $\sqrt{s} = 900, 2360$ , and  $7000$  GeV in the central pseudorapidity region  $|\eta| < 1$  in the sample  $n_{ch} > 0$ . (b) MD of charged particles measured by the ATLAS Collaboration [14] at the energies  $\sqrt{s} = 900$  and  $7000$  GeV in the pseudorapidity region  $|\eta| < 2.5$  with the selection  $p_T > 100$  MeV and  $n_{ch} \geq 2$ . Data are accumulated in the neighbouring even and odd bins and multiplied by the indicated factors. The lines represent description of the data with GHD.

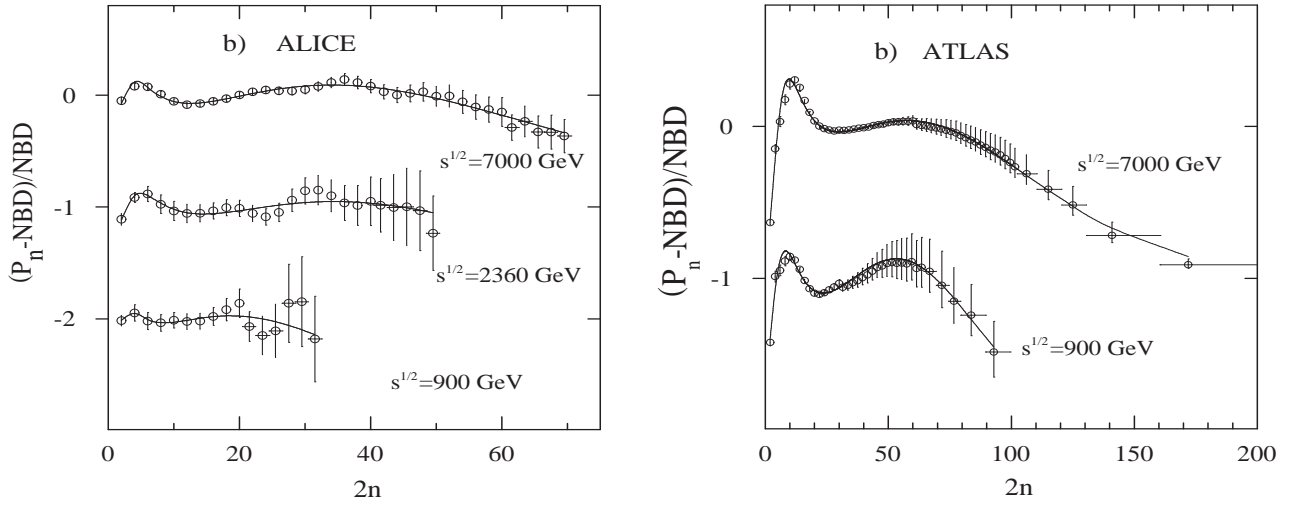


FIG. 7: (a) The relative residues of the data from Fig.6(a) with respect to the NBD parametrization. (b) The relative residues of the data from Fig.6(b) with respect to the NBD parametrization. The residues are shifted by unity for different  $\sqrt{s}$ . The lines represent description of the data with GHD.

At the same time the shoulder widens and its maximum moves towards larger multiplicity. On the other hand one can see from Figs. 4(b) and 5(b) that, for the smallest window  $|\eta| < 0.5$ , the multiplicity structure vanishes and the residues of MD with respect to the NBD parametrization become flat at both these energies. This is in accord with the conclusions of Ref. [7], namely that at  $\sqrt{s} = 900$  and 2360 GeV the experimentally measured multiplicity distributions are well described by NBD for  $\eta_c = 0.5$ .

The ALICE Collaboration presented data [13] on MD of charged particles in  $pp$  collisions at the energies  $\sqrt{s} = 900$ , 2360, and 7000 GeV. Figure 6(a) shows the experimentally measured MD collected in the neighbouring even and odd bins in multiplicity (11) in the central pseudorapidity region  $|\eta| < 1$ . The data are from an event class where at least one charged particle in the measured pseudorapidity range is required. The depicted distributions are multiplied by the powers of 0.2 for different  $\sqrt{s}$ . The corresponding relative residues with respect to the NBD parametrization are presented in Fig. 7(a). The residues are mutually shifted by unity for different energies. The full lines represent description of the ALICE data by GHD. One can see from Fig. 7(a) that data on MD for  $|\eta| < 1$  at the energy  $\sqrt{s} = 900$  GeV can be well described by NBD. At  $\sqrt{s} = 2360$  GeV, NBD is still good description of data with the exception at low  $n$  where a peaky structure begins to emerge. The peak at low multiplicity is clearly visible especially at  $\sqrt{s} = 7000$  GeV. One can see from Fig. 7(a) that NBD overestimates experimental data for high multiplicities ( $n > 55$ ) at this super high energy, as was already observed in Ref. [13].

The ATLAS Collaboration measured the charged-particle MD [14] in different phase-space regions for various multiplicity cuts at three LHC energies. The most inclusive phase-space region covered by the measurements corresponds to the conditions  $|\eta| < 2.5$ ,  $p_T > 100$  MeV and  $n_{ch} \geq 2$ . We analyse the ATLAS data obtained under the above  $\eta_c$  and  $p_T$  selections at  $\sqrt{s} = 900$  and 7000 GeV. Figure 6(b) shows the experimentally measured MD collected in the neighbouring even and odd bins in multiplicity (11). The distribution at  $\sqrt{s} = 900$  GeV is multiplied by the factor of 0.2. Figure 7(b) shows the corresponding relative residues with respect to the NBD parametrization. The residues at  $\sqrt{s} = 900$  GeV are shifted down by the factor of unity. The full lines represent approximation of the ATLAS data by GHD. The distinct peak at low multiplicities in the ATLAS data represent stringent criterion for description of the whole shape of the distribution. Values of the parameters and processes included in GHD are strongly restricted by the peak's position, its width and height as well as by the form of the shoulder at high  $n$ . The four parametric GHD accounts for smooth transition from the peak region to the shoulder at high multiplicities. Both structures in the ATLAS data are measured at such level of the experimental errors which exclude other processes to be present

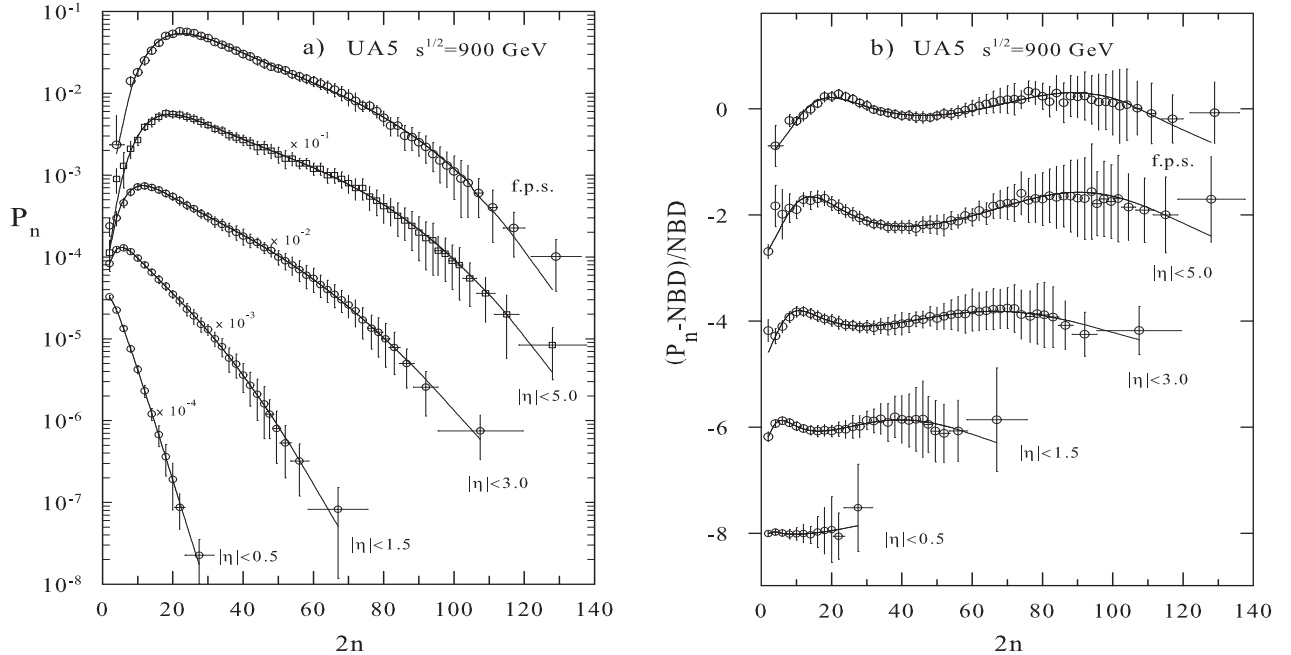


FIG. 8: (a) MD of charged particles in the full phase-space and in the limited phase-space regions from the NSD  $pp$  collisions at  $\sqrt{s} = 900$  GeV. The data [24] are accumulated in the neighbouring even and odd bins and multiplied by the indicated factors. (b) The corresponding relative residues with respect to the NBD parametrization. The residues are shifted mutually by the factor of two for different  $\eta_c$ . The lines represent description of the data by GHD.

in GHD but those considered. Beside this, we have checked that application of GHD to the MD of particle pairs is substantial because when applied to the distribution of all charged particles, the form of data is not reproduced correctly. The measurements performed by the CMS, ALICE, and ATLAS Collaborations show that the peaky structure of MD is clearly seen in  $pp$  collisions in the limited phase-space regions at the LHC energies. The structure becomes more distinct with the increasing width of the pseudorapidity window and is most pronounced at the highest energy  $\sqrt{s} = 7000$  GeV.

A similar trend in the pseudorapidity dependence of MD is visible in data [24] measured by the UA5 Collaboration in the NSD  $p\bar{p}$  collisions at  $\sqrt{s} = 900$  GeV. Figure 8(a) shows the UA5 data collected in the neighbouring even and odd bins in multiplicity (11) in the full phase-space and in four smaller pseudorapidity regions. The depicted distributions are multiplied by the powers of 0.1 for different  $\eta_c$ . Figure 8(b) shows the corresponding relative residues with respect to the NBD parametrization. The residues in the smaller pseudorapidity windows are mutually shifted down by the factor of two. The full lines represent description of the UA5 data by GHD. Starting from the window  $|\eta| < 1.5$  a small peak at low multiplicity emerges in the shape of MD. It evolves with the window size and becomes best visible in the full phase-space. As can be seen from Fig. 8(b), the residues with respect to NBD are perfectly flat in the smallest window  $|\eta| < 0.5$  meaning that NBD describes MD in this region well.

### B. Multiplicity distribution in $e^+e^-$ annihilations

The study of multihadron production in  $e^+e^-$  annihilations can provide additional information on correlation structures which are encoded in MD in an integrated form. The qualitative picture of MD of charged hadrons in leptonic processes differs in many properties from  $pp/p\bar{p}$  interactions. The average multiplicities are higher and the distributions are narrower in  $e^+e^-$  annihilation in comparison with the hadron collisions at the same energies. At phenomenological level, a comparison of both types of the interactions may reveal which features reflect difference in the initial state and which are intrinsic to the parton-hadron transitions.

Using formula (10) for GHD, we studied the inclusive samples of MD of charged hadrons produced in  $e^+e^-$  annihilations in the full phase-space at various collision energies  $\sqrt{s}$ . Similarly as in the previous section, GHD is applied to the distribution of particle pairs for all multiplicities  $n \geq n_0$ . The value of  $n_0$  is the minimal number of the charged particle pairs measured in experiment. The results of the analysis are presented in Table II and Figs. 9-10. We have analysed data on MD of charged particles obtained by the OPAL Collaboration at the centre-of-mass energies of  $\sqrt{s} = 172, 183$ , and  $189$  GeV [34]. The data with high statistical precision correspond to the energy region sufficiently far beyond  $Z^0$  peak. The three data samples are measured in the multiplicity range which begins with  $n_{ch} = 8$  i.e. with  $n_0 = 4$  particle pairs. The analysis includes also data on MD measured by the OPAL Collaboration at lower energies,  $\sqrt{s} = 161$  GeV [35],  $\sqrt{s} = 133$  GeV [36], and at the energy of  $Z^0$  peak,  $\sqrt{s} = 91$  GeV [37]. The application of GHD to the OPAL data shows that the parameter  $\beta_0/\beta_2$  is compatible with zero and, therefore, it was set to null in this high energy region. In such a case, GHD becomes three parameter distribution for which the recurrence relation (1) takes the form

$$\frac{(n+1)P_{n+1}}{P_n} = \frac{\bar{\alpha}_0}{n(n-1)} + \bar{\alpha}_2 + \bar{\alpha}_3(n-2), \quad \bar{\alpha}_i \equiv \alpha_i/\beta_2. \quad (12)$$

In this limit the distribution reflects relatively sharp increase of  $P_n$  at low  $n \geq n_0$  typical for  $e^+e^-$  annihilations at high energies and accounts for a "negative binomial tail" at large multiplicities.

The relative residues of MD of charged particles measured by the OPAL Collaboration with respect to the description of the data by GHD with three parameters (12) are depicted in Fig. 9(a). The residues are nearly zero reflecting acceptable parametrization of the experimental data. Similar holds for the data [38] obtained by the ALEPH Collaboration at the energy  $\sqrt{s} = 91$  GeV (see Table II). As shown in Ref. [17], a good description of the OPAL data can be obtained also by GMD characterized by the recurrence factor (5). An exception represent data on MD measured by the DELPHI Collaboration at the energy of  $Z^0$  peak in the sense that their description requires a non-zero value of the parameter  $\beta_0/\beta_2$ . As seen from Table II, this parameter is required also by data at lower energies. The relative residues of MD of charged particles measured by the DELPHI [39], AMY [40], TASSO [41], and HRS [42] Collaborations with respect to the four parametric GHD are depicted in Fig. 9(b). In all cases a good description is obtained.

We analysed also data [43] on MD in  $e^+e^-$  annihilations measured by the MARK I Collaboration in the low energy region. The application of GHD to the multiplicity data for  $\sqrt{s} < 10$  GeV gives negative values of the parameters  $\alpha_3/\beta_2$  and  $\alpha_2/\beta_2$  with an over-parametrized description. Therefore we set  $\alpha_3 = \alpha_2 = 0$  at these energies. In that case, similarly as for  $pp$  collisions at very low energies, MD in  $e^+e^-$  annihilation can be characterized by the recurrence (1) with

$$g^{-1}(n) = \bar{\beta}_0 + \bar{\beta}_2 n(n-1), \quad \bar{\beta}_i \equiv \beta_i/\alpha_0. \quad (13)$$

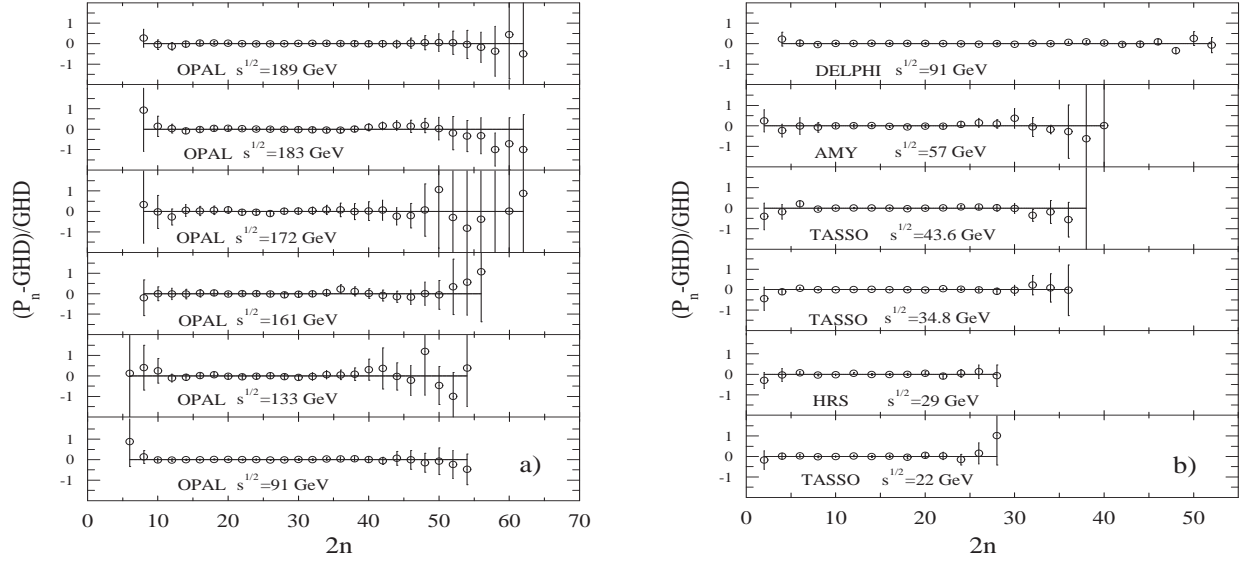


FIG. 9: The relative residues of MD of charged particles produced in  $e^+e^-$  annihilation in the full phase-space with respect to description by GHD. (a) The data measured by the OPAL Collaboration at  $\sqrt{s} = 189, 183, 172$  GeV are from Ref. [34], at  $\sqrt{s} = 161$  GeV from Ref. [35], at  $\sqrt{s} = 133$  GeV from Ref. [36], and at  $\sqrt{s} = 91$  GeV from Ref. [37]. (b) The data measured by the DELPHI Collaboration at  $\sqrt{s} = 91$  GeV are from Ref. [39]. The combined data measured by the AMY Collaboration at  $\sqrt{s} = 57$  GeV are from Ref. [40]. The data measured by the TASSO Collaboration at  $\sqrt{s} = 43.6, 34.8$ , and  $22$  GeV are from Ref. [41]. The data measured by the HRS Collaboration at  $\sqrt{s} = 29$  GeV are from Ref. [42].

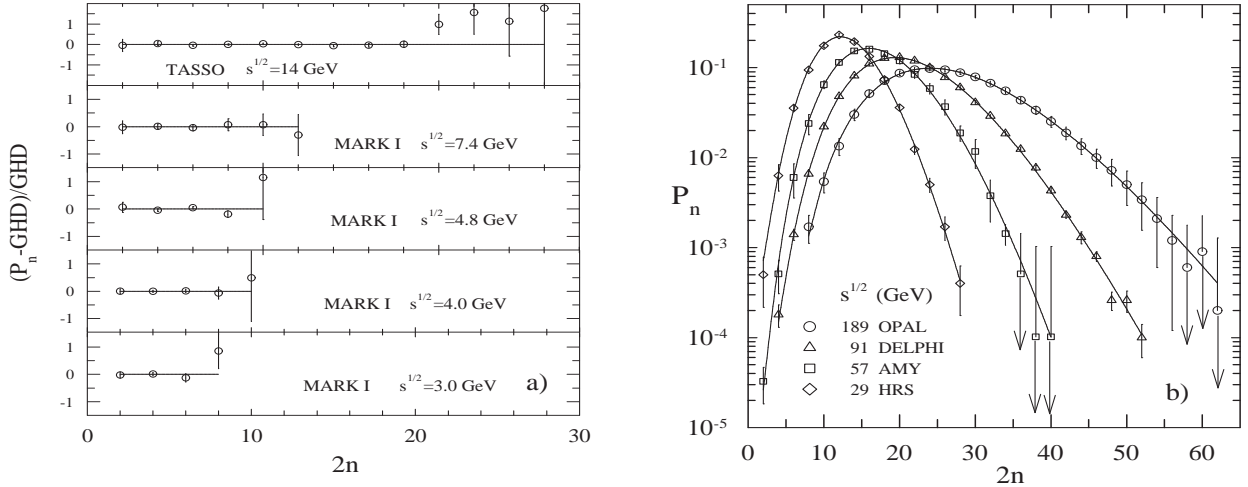


FIG. 10: (a) The relative residues of MD of charged particles produced in  $e^+e^-$  annihilation in the full phase-space with respect to description by GHD. The data measured by the TASSO Collaboration at  $\sqrt{s} = 14$  GeV are from Ref. [41]. The data measured by the MARK I Collaboration at  $\sqrt{s} = 7.4, 4.8, 4.0$ , and  $3.0$  GeV are from Ref. [43]. (b) The energy dependence of MD of charged particles produced in  $e^+e^-$  annihilation in the full phase-space. The depicted data from the OPAL [34], DELPHI [39], AMY [40], and HRS [42] Collaborations were measured at the energies  $\sqrt{s} = 189, 91, 57$ , and  $22$  GeV, respectively. The lines represent description of the data by GHD.

Because of the non-zero values of  $\bar{\beta}_2$  in (13), GHD is narrower than Poisson distribution in this region. Figure 10(a) shows the relative residues of MD with respect to GHD at low energies. A summarizing illustration of the description of MD of charged particles produced in  $e^+e^-$  annihilations at some energies is presented in Fig. 10(b). The full lines represent GHD with parameters quoted in Table II.

TABLE II: The results of analysis of MD of the charged particle pairs in  $e^+e^-$  annihilations in the full phase-space by GHD. The minimal number of the pairs is  $n_0$ . If not quoted, the corresponding parameter of GHD was set to null. The errors correspond to the quadratic sum of the statistical and systematic uncertainties of data when both are published.

$\sqrt{s}$ (GeV)		GHD					$\chi^2/\text{NDF}$
		$n_0$	$\alpha_0/\beta_2$	$\alpha_2/\beta_2$	$\alpha_3/\beta_2$	$\beta_0/\beta_2$	
189	OPAL	4	$163 \pm 34$	$6.8 \pm 0.8$	$0.47 \pm 0.05$	-	1.9/25
183	OPAL	4	$344 \pm 61$	$3.0 \pm 1.3$	$0.67 \pm 0.07$	-	6.5/25
172	OPAL	4	$123 \pm 108$	$8.5 \pm 2.7$	$0.29 \pm 0.17$	-	3.0/25
161	OPAL	4	$130 \pm 55$	$6.8 \pm 1.5$	$0.40 \pm 0.09$	-	3.0/22
133	OPAL	3	$198 \pm 69$	$4.3 \pm 1.8$	$0.54 \pm 0.12$	-	3.9/22
91	OPAL	3	$131 \pm 17$	$6.1 \pm 0.5$	$0.33 \pm 0.04$	-	3.1/22
91	DELPHI	2	$192 \pm 41$	$6.2 \pm 0.4$	$0.31 \pm 0.03$	$5.4 \pm 2.6$	11.9/21
91	ALEPH	2	$127 \pm 39$	$5.9 \pm 1.4$	$0.33 \pm 0.10$	-	3.2/23
57	AMY	1	$92 \pm 33$	$6.8 \pm 1.0$	$0.02 \pm 0.09$	$1.8 \pm 1.3$	4.5/16
43.6	TASSO	1	$141 \pm 42$	$5.7 \pm 0.2$	-	$9.2 \pm 4.3$	7.3/16
34.8	TASSO	1	$191 \pm 49$	$1.9 \pm 1.1$	$0.28 \pm 0.10$	$12.0 \pm 4.1$	6.6/14
29	HRS	1	$153 \pm 76$	$2.7 \pm 2.3$	$0.05 \pm 0.23$	$8.4 \pm 5.6$	5.0/10
22	TASSO	1	$77 \pm 36$	$2.6 \pm 1.5$	$0.11 \pm 0.18$	$4.3 \pm 3.0$	2.2/10
14	TASSO	1	$37 \pm 6$	$2.3 \pm 0.2$	-	$2.1 \pm 0.7$	10.3/10
7.4	MARK I	1	$40 \pm 16$	-	-	$11.9 \pm 6.2$	0.4/4
4.8	MARK I	1	$7.3 \pm 0.7$	-	-	$1.1 \pm 0.3$	5.0/3
4.0	MARK I	1	$8.1 \pm 1.2$	-	-	$2.2 \pm 0.5$	0.2/3
3.0	MARK I	1	$5.3 \pm 1.8$	-	-	$2.2 \pm 0.9$	2.6/2

#### IV. DISCUSSION

The motivation of the present study of multiple production originates from the experimental observation that in  $pp/p\bar{p}$  interactions at high energies a structure in the charged particle MD emerges both in the full phase-space and in the limited phase-space regions. We concentrate in obtaining a plausible description of the observed structure which is distinctly visible in new data from the LHC in the super high energy domain. The phenomenological analysis is based on a scenario of multiparticle production in terms of parton cascade processes. The proposed approach aims to grasp some qualitative features of parton to hadron transitions which may be important at the end of the parton cascading. The observable shape of MD is assumed to be influenced mostly by the soft particles produced in the final stages of the cascade development. Besides the ordinary birth ( $0 \rightarrow 1$ ) and death ( $1 \rightarrow 0$ ) process, we consider the multiparton incremental ( $2 \rightarrow 3$ ), ( $3 \rightarrow 4$ ) and decremental ( $3 \rightarrow 2$ ) recombination processes which are supposed to contribute significantly to the multiplicity build up. Such kind of two and three parton recombination interactions in the final stage of the cascade evolution can be justified by the physical requirements of color neutralization and reaching of an approximate "momenta uniformity" at hadronization.

The phenomenological background of data description relies on DD evolution equations which include the terms corresponding to the suggested processes. A stationary solution of the equations gives the recurrence relation (10) defining a distribution which we refer to as GHD. The essential ingredients of the analysis are four parameters of GHD which are the ratios  $\alpha_0/\beta_2$ ,  $\alpha_2/\beta_2$ ,  $\alpha_3/\beta_2$ , and  $\beta_0/\beta_2$  constructed from the rates  $\alpha_i$  and  $\beta_i$  of the incremental and decremental parton cascade processes, respectively. The energy dependence of the parameters in the full phase-space which follows from the performed analysis is shown in Figs. 11 and 12. The empty symbols represent the values obtained from data on MD in  $pp/p\bar{p}$  interactions. The full symbols correspond to  $e^+e^-$  annihilations. The regular behaviour of all four parameters is guaranteed by the non-zero values of  $\beta_2$ . It means that the recombination process ( $3 \rightarrow 2$ ) is present in both reactions at all energies. The ratios  $\alpha_0/\beta_2$  and  $\beta_0/\beta_2$  reflect features of data connected with the different initial state in the lepton and hadron collisions. They are proportional to the rates  $\alpha_0$  and  $\beta_0$  of the immigration and death processes governed by the interactions of partons with the rest of the system as a whole. We will refer to them as parameters of the I. type. As one can see from Fig. 11(a), the parameter  $\alpha_0/\beta_2$  increases with  $\sqrt{s}$  for both reactions. This means that an increase in the collision energy results in the relative enhancement of the

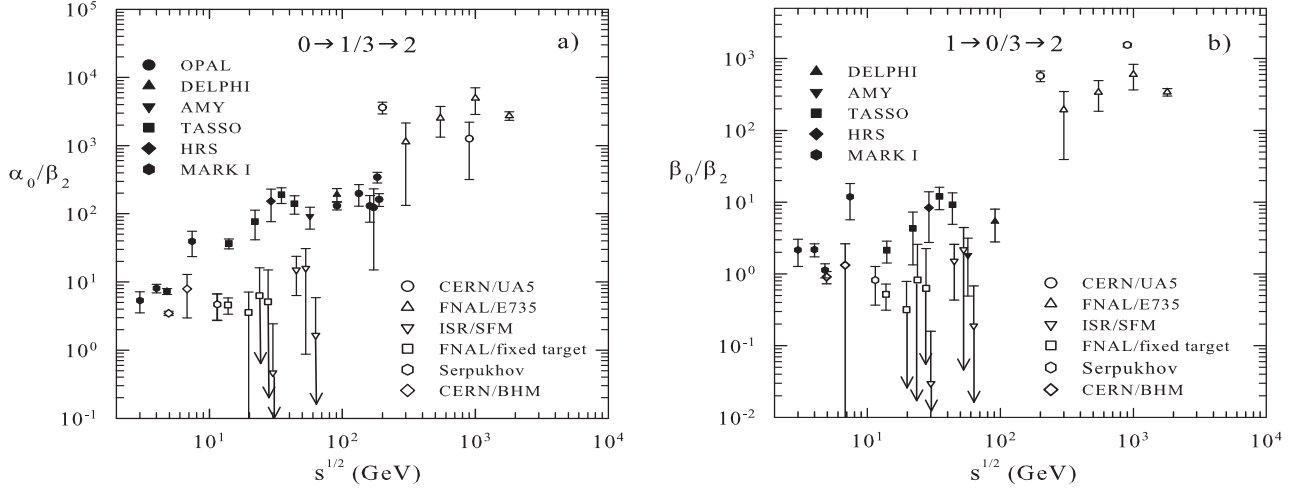


FIG. 11: The energy dependence of the parameters  $\alpha_0/\beta_2$  and  $\beta_0/\beta_2$  of GHD obtained from the analysis of data on MD in the full phase-space. The full and empty symbols correspond to  $e^+e^-$  and  $pp/pp\bar{p}$  interactions, respectively. (a) Ratio of the corresponding rates for the process  $0 \rightarrow 1$  of parton immigration and the process  $3 \rightarrow 2$  of parton recombination. (b) Ratio of the corresponding rates for the process  $1 \rightarrow 0$  of parton absorption and the process  $3 \rightarrow 2$  of parton recombination.

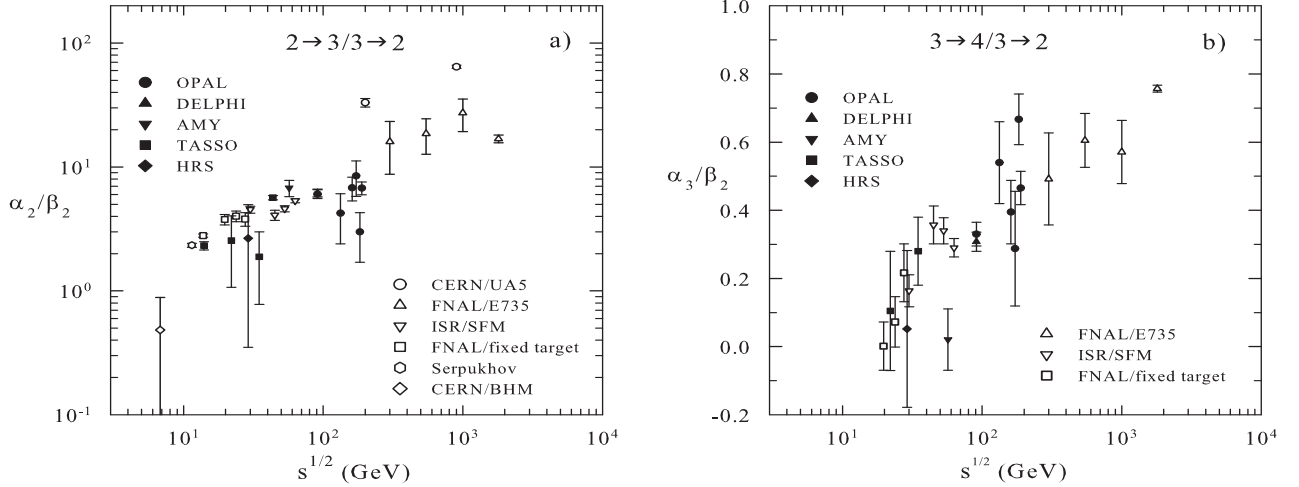


FIG. 12: The energy dependence of the parameters  $\alpha_2/\beta_2$  and  $\alpha_3/\beta_2$  of GHD obtained from the analysis of data on MD in the full phase-space. The full and empty symbols correspond to  $e^+e^-$  and  $pp/pp\bar{p}$  interactions, respectively. (a) Ratio of the recombination rates for the processes  $2 \rightarrow 3$  and  $3 \rightarrow 2$ . (b) Ratio of the recombination rates for the processes  $3 \rightarrow 4$  and  $3 \rightarrow 2$ .

parton immigration ( $0 \rightarrow 1$ ) with respect to the three parton decremental recombination ( $3 \rightarrow 2$ ). Figure 11(b) shows similar trend in the parameter  $\beta_0/\beta_2$  for  $pp/pp\bar{p}$  collisions. The relative increase of the rate  $\beta_0$  with  $\sqrt{s}$  points to the intensive absorption of partons in the bulk of the expanding system formed in hadron collisions at high energies. A different picture is foreseen in  $e^+e^-$  annihilations. Here the parameter  $\beta_0/\beta_2$  reaches a maximum at  $\sqrt{s} \simeq 40$  GeV and beyond the energy of  $Z^0$  peak it drops to zero (see Table II). This suggests that, in contrast to the hadron collisions, the parton absorption becomes negligible in the  $e^+e^-$  annihilations at high energies.

Another difference in the behaviour of the parameters of the I. type for the lepton and hadron collisions is in their absolute values. In the region below  $\sqrt{s} \simeq 40$  GeV, both parameters  $\alpha_0/\beta_2$  and  $\beta_0/\beta_2$  are larger for  $e^+e^-$  annihilations in comparison with  $pp/pp\bar{p}$  interactions. There are indications from Figs. 11 and 12 that, at high energies, this tendency may be opposite. A reason for such a behaviour may be influence of jets on the multiplicity structure. While in the  $e^+e^-$  annihilations at low energies the immigration rate  $\alpha_0$  stemming from two (or few) jets prevails the parton immigration in the hadron collisions, the multitude of minijets at high energies would result in much larger  $\alpha_0$  in the  $pp/pp\bar{p}$  interactions. This in turn would lead to the higher absorption rate  $\beta_0$  in the hadron collisions giving the partons more probability to be melted conversely in the complex system with many minijets again.

As seen from Figs. 11 and 12, there exists a region in which the parameters  $\alpha_0/\beta_2$  and  $\beta_0/\beta_2$  can be relatively small within the errors indicated. The region corresponds to the  $pp$  interactions in the energy interval  $\sqrt{s} \sim 20 - 60$  GeV. The small values of  $\alpha_0$  and  $\beta_0$  mean that GHD depends mostly on the parameters  $\alpha_2/\beta_2$  and  $\alpha_3/\beta_2$ . In such case the data can be relatively well approximated by NBD except for a few low values of  $n$  (see Fig. 2(b)).

The energy dependence of  $\alpha_2/\beta_2$  and  $\alpha_3/\beta_2$  is shown in Fig. 12. The ratios depend only on the rates of recombination processes which are assumed to be active at the stage of parton-hadron conversions. The parameters characterize features of data connected with a breakdown of confinement and onset of hadronization. We denote  $\alpha_2/\beta_2$  and  $\alpha_3/\beta_2$  as parameters of II. type. Within the errors indicated, both parameters reveal approximately the same energy dependence common for  $e^+e^-$  and  $pp/p\bar{p}$  collisions. Exceptions make the values for UA5 data [24] which result from discrepancies at high multiplicities pointed out in Ref. [10]. As seen from Tables I, II and Fig. 12(a), the parameter  $\alpha_2/\beta_2$  has a threshold in the region  $\sqrt{s} \sim 7$  GeV. Afterwards it becomes larger than unity and continues in rapid growth at high energies. This means that, with increasing  $\sqrt{s}$ , the rate of the recombination process ( $2 \rightarrow 3$ ) prevails still more and more the rate of the inverse process ( $3 \rightarrow 2$ ). The parameter  $\alpha_3/\beta_2$  has a threshold in the region  $\sqrt{s} \sim 20$  GeV. It grows with the energy and reaches the value of 0.6 at  $\sqrt{s} \sim 1$  TeV.

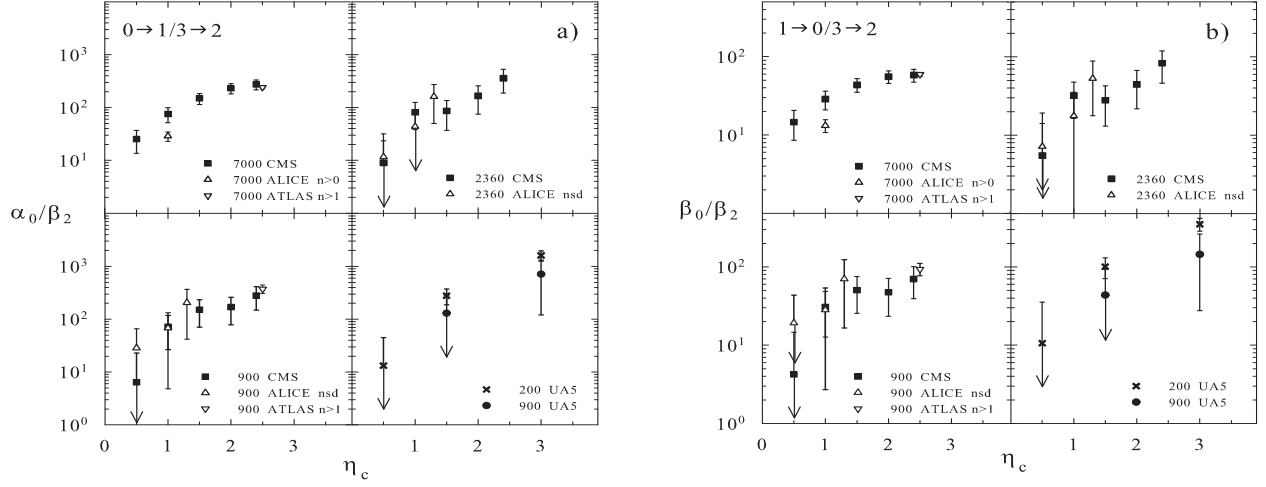


FIG. 13: The pseudorapidity dependence of the parameters  $\alpha_0/\beta_2$  and  $\beta_0/\beta_2$  of GHD obtained from analysis of MD in  $pp/p\bar{p}$  interactions at different  $\sqrt{s}$ . (a) Ratio of the corresponding rates for the process  $0 \rightarrow 1$  of parton immigration and the process  $3 \rightarrow 2$  of parton recombination. (b) Ratio of the corresponding rates for the process  $1 \rightarrow 0$  of parton absorption and the process  $3 \rightarrow 2$  of parton recombination.

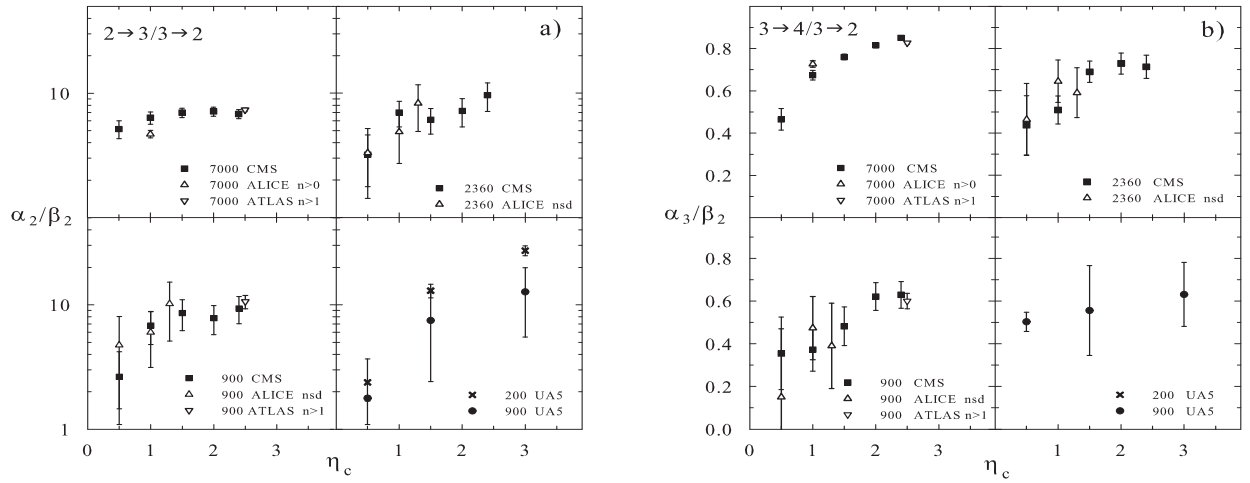


FIG. 14: The pseudorapidity dependence of the parameters  $\alpha_2/\beta_2$  and  $\alpha_3/\beta_2$  of GHD obtained from analysis of MD in  $pp/p\bar{p}$  interactions at different  $\sqrt{s}$ . (a) Ratio of the recombination rates for the processes  $2 \rightarrow 3$  and  $3 \rightarrow 2$ . (b) Ratio of the recombination rates for the processes  $3 \rightarrow 4$  and  $3 \rightarrow 2$ .

In contrast to the parameters of I. type, the parameters of II. type reflect features of multiplicity production which are common to the  $e^+e^-$  and  $pp/p\bar{p}$  interactions. The analysis suggests that two and three parton recombination processes may be part of an intrinsic property of the parton-hadron transitions. Physical justification for such an idea may be connected with the processes of color neutralization.

Experimental data on MD in the central pseudorapidity windows  $|\eta| < \eta_c$  allow us to study the behaviour of the parton processes in the limited phase-space regions. The structure of MD observed in the hadron collisions in the full phase-space demonstrate itself distinctly in the limited windows in pseudorapidity if the collision energy is sufficiently high. This allows more reliable determination of the ratios of the corresponding rates of single processes in dependence on the window size. The fine structure of MD is visible even for small  $\eta_c = 0.5$  in  $pp$  collisions at  $\sqrt{s} = 7000$  GeV. The data at this energy give strongest restriction on the values of the parameters in the small pseudorapidity range. The dependence of the ratios  $\alpha_0/\beta_2$ ,  $\alpha_2/\beta_2$ ,  $\alpha_3/\beta_2$ , and  $\beta_0/\beta_2$  on  $\eta_c$  is depicted in Figs. 13 and 14. The symbols represent values of the parameters obtained from the analysis of data measured by the CMS, ALICE, ATLAS, and UA5 Collaborations at different energies. For clarity reasons, every figure is divided into four panels. Three panels show the values obtained from analysis of data measured at the LHC at  $\sqrt{s} = 7000, 2360$ , and  $900$  GeV, respectively. The values corresponding to the UA5 data are shown on the fourth panel.

One can see from Fig. 13 that  $\alpha_0/\beta_2$  and  $\beta_0/\beta_2$  increase with  $\eta_c$  at all displayed energies. Both parameters reveal weak energy dependence in the depicted  $\eta_c$  region. With the increasing window size, the value of  $\alpha_0$  becomes still larger than  $\beta_0$ . This means that the rate of the immigration process ( $0 \rightarrow 1$ ) grows faster with pseudorapidity than the rate of the parton absorption ( $1 \rightarrow 0$ ). Except for the energy  $\sqrt{s} = 7000$  GeV, the parameters  $\alpha_0/\beta_2$  and  $\beta_0/\beta_2$  can be relatively small for  $\eta_c = 0.5$  within the errors indicated. In such a case GHD depends effectively on two parameters of the II. type and can be approximated by NBD. This is seen in Figs. 4(b), 5(b), and 8(b) where good approximation of data by NBD at  $\sqrt{s} = 2360$  and  $900$  GeV for  $\eta_c = 0.5$  is demonstrated. Such conclusion is in accord with the resume made in Ref. [7]. As shown in Fig. 13, the errors of  $\alpha_0/\beta_2$  and  $\beta_0/\beta_2$  at  $\sqrt{s} = 7000$  GeV exclude small values of these parameters even for  $\eta_c = 0.5$ . This is why the data cannot be well approximated by NBD. The statement rephrases the fact that structure of MD stays beyond the NBD description in this region (see lowest part of Fig.3(b)).

The pseudorapidity dependence of the parameters  $\alpha_2/\beta_2$  and  $\alpha_3/\beta_2$  is shown in Fig. 14. The ratio  $\alpha_2/\beta_2$  reveals growing tendency with  $\eta_c$  and flattens at  $\sqrt{s} = 7000$  GeV. This observation suggests importance of the two parton incremental recombination process ( $2 \rightarrow 3$ ) in the small pseudorapidity windows at this ultra high energy. On the contrary, three parton incremental recombination ( $3 \rightarrow 4$ ) falls for small  $\eta_c$ , as shown in the upper left panel in Fig.14(b). The growing tendency of  $\alpha_3/\beta_2$  with  $\eta_c$  is seen in the LHC data at all quoted energies.

## V. CONCLUSIONS

Charged particle multiplicity distributions in  $pp/p\bar{p}$  collisions have been studied including new data from the LHC. The analysis comprises MD in the full phase-space as well in the limited windows in pseudorapidity. At high energies the distributions show a relatively narrow peak at small multiplicities and a shoulder in the tail.

A phenomenological description of the observed structure was proposed. Using techniques based on the solution of DD evolution equations relevant for the stochastico-physical picture of particle production a simple formula (10) for the probabilities of the secondary produced multiplicity has been obtained in a stationary regime. The basic ingredients of the scenario are the elementary immigration and absorption of partons and the processes of particle recombination. We considered two and there particle incremental ( $2 \rightarrow 3$ ), ( $3 \rightarrow 4$ ) and three particle decremental ( $3 \rightarrow 2$ ) recombinations. Physical justification for existence of such kind of processes may be connected with the requirements of color neutralization at the end of the parton cascade and reaching of an approximate "momenta uniformity" of the soft particles at hadronization. The features such as two and three parton recombination allow to change particle number, exchange particle momenta and neutralize color repeatedly just before the conversions into the observable hadrons. The corresponding solution of the higher order equation for the generating function based on the recombination processes exhibit qualitative properties which are absent in the first order.

This allowed a quantitative description of the complex structure of data on MD in  $pp/p\bar{p}$  collisions both in the full phase-space and in the limited pseudorapidity windows. The phenomenological formula (GHD) was applied to the description of the charged particle distributions in  $e^+e^-$  annihilations at different energies  $\sqrt{s}$ . A good agreement with data was obtained. The dependence of the four parameters of GHD on the energy and pseudorapidity was discussed. The behaviour of some parameters reveals a universal character which is independent of the reaction type while some other parameters depend on it. It was shown that the incremental recombination processes play an increasingly large role in the multiplicity production as the collision energy increases.

Within the approach used and on the basis of the studied material we conclude that data on MD indicate existence of certain type of recombination processes correlating particle degrees of freedom which manifest itself at high energies.



### Acknowledgments

The investigations have been supported by the IRP AVOZ10480505, by the Ministry of Education, Youth and Sports of the Czech Republic grant LA08002.

### Appendix A

The system of the evolution rate equations (6) can be solved analytically in a stationary regime. The stationary solution for the generation function satisfies the differential equation (8). Introducing the substitution

$$z = \frac{\alpha_3}{\beta_2} w \quad (14)$$

the equation for  $Q(w) = F(z)$  becomes

$$(z^3 - z^2) \frac{d^3 F(z)}{dz^3} + \frac{\alpha_2}{\alpha_3} z^2 \frac{d^2 F(z)}{dz^2} - \frac{\beta_0}{\beta_2} \frac{dF(z)}{dz} + \frac{\alpha_0}{\alpha_3} F(z) = 0. \quad (15)$$

It can be rewritten into the known form

$$\left[ \left( z \frac{d}{dz} + a_1 \right) \left( z \frac{d}{dz} + a_2 \right) \left( z \frac{d}{dz} + a_3 \right) - \left( z \frac{d}{dz} + b_1 - 1 \right) \left( z \frac{d}{dz} + b_2 - 1 \right) \right] F(z) = 0 \quad (16)$$

for the generalized hypergeometric function  ${}_3F_2(a_1, a_2, a_3; b_1, b_2; z)$ . Exploiting the decomposition of  ${}_3F_2(z)$  into the power series of its argument the recurrence relation (1) can be written as follows

$$\frac{(n+1)P_{n+1}}{P_n} = \frac{(a_1+n)(a_2+n)(a_3+n)}{(b_1+n)(b_2+n)} \frac{\alpha_3}{\beta_2}. \quad (17)$$

Here we used (14) and the standard relation for calculating the probabilities from the generating function,

$$P_n = \frac{1}{n!} \left. \frac{d^n Q}{dw^n} \right|_{w=0}. \quad (18)$$

Now, the recurrence relation (17) remains to be expressed in terms of the rate parameters  $\alpha_i$  and  $\beta_i$ . For this purpose we perform the differentiations in (16) and obtain

$$\begin{aligned} & (z^3 - z^2) \frac{d^3 F(z)}{dz^3} + z [(3 + a_1 + a_2 + a_3)z - (1 + b_1 + b_2)] \frac{d^2 F(z)}{dz^2} \\ & + [(1 + a_1 + a_2 + a_3 + a_1 a_2 + a_1 a_3 + a_2 a_3)z - b_1 b_2] \frac{dF(z)}{dz} + a_1 a_2 a_3 F(z) = 0. \end{aligned} \quad (19)$$

The comparison of the coefficients in the equations (15) and (19) gives

$$\begin{aligned} 1 + a_1 + a_2 + a_3 + a_1 a_2 + a_1 a_3 + a_2 a_3 &= 0, \\ 3 + a_1 + a_2 + a_3 &= \frac{\alpha_2}{\alpha_3}, \quad a_1 a_2 a_3 = \frac{\alpha_0}{\alpha_3} \end{aligned} \quad (20)$$

and

$$1 + b_1 + b_2 = 0, \quad b_1 b_2 = \frac{\beta_0}{\beta_2}. \quad (21)$$

The first system of equations represents the correspondence between the sets of parameters  $a_i$  and  $\alpha_i$ . The second system connects  $b_i$  and  $\beta_i$ . After performing multiplication on the right hand side of (17) and exploiting relations (20) and (21), one obtains directly the recurrence relation (10).

In the analysis of data we deal with the number of particle pairs  $n$ . The minimal number of the pairs  $n_0$  is always greater than null. For the NSD  $pp/p\bar{p}$  collisions we take  $n_0 = 1$  in all cases. The values of  $n_0$  for  $e^+e^-$  annihilations are shown in Table II. The recurrence relation (10) begins always with  $n_0$  and the obtained values of  $P_n$  are renormalized. The corresponding generating function reads  $Q(w) = cw^{n_0} {}_3F_2(z)$ .

## Appendix B

TABLE III: The results of analysis of MD of the charged particle pairs in  $pp$  collisions in the limited phase-space regions  $|\eta| < \eta_c$  by the negative binomial distribution (NBD) and generalized hypergeometric distribution (GHD). The data measured by the CMS Collaboration are taken from Ref. [3].

$\sqrt{s}$ (GeV)	$\eta_c$	NBD			GHD				
		k	q	$\chi^2/\text{NDF}$	$\alpha_0/\beta_2$	$\alpha_2/\beta_2$	$\alpha_3/\beta_2$	$\beta_0/\beta_2$	$\chi^2/\text{NDF}$
7000	2.4	$1.56 \pm 0.03$	$0.910 \pm 0.001$	89.4/67	$(2.7 \pm 0.6)10^2$	$6.8 \pm 0.6$	$0.85 \pm 0.01$	$58 \pm 11$	6.4/65
	2.0	$1.66 \pm 0.03$	$0.888 \pm 0.001$	140.9/61	$(2.3 \pm 0.5)10^2$	$7.1 \pm 0.6$	$0.82 \pm 0.01$	$56 \pm 10$	7.4/59
	1.5	$1.72 \pm 0.03$	$0.851 \pm 0.002$	143.5/54	$(1.5 \pm 0.4)10^2$	$7.0 \pm 0.6$	$0.76 \pm 0.01$	$44 \pm 9$	3.9/52
	1.0	$1.68 \pm 0.04$	$0.793 \pm 0.003$	92.4/38	$76 \pm 24$	$6.4 \pm 0.7$	$0.67 \pm 0.02$	$29 \pm 8$	1.9/36
	0.5	$1.69 \pm 0.07$	$0.652 \pm 0.006$	51/20	$25 \pm 12$	$5.2 \pm 0.9$	$0.47 \pm 0.05$	$15 \pm 6$	1.7/18
2360	2.4	$1.99 \pm 0.08$	$0.858 \pm 0.004$	30.9/40	$(3.6 \pm 1.7)10^2$	$9.6 \pm 2.5$	$0.71 \pm 0.06$	$83 \pm 37$	9.8/38
	2.0	$1.89 \pm 0.09$	$0.840 \pm 0.005$	22.2/33	$(1.7 \pm 0.9)10^2$	$7.2 \pm 1.8$	$0.73 \pm 0.06$	$45 \pm 23$	8.6/31
	1.5	$1.90 \pm 0.09$	$0.797 \pm 0.005$	17.7/27	$86 \pm 50$	$6.1 \pm 1.4$	$0.69 \pm 0.05$	$28 \pm 15$	4.4/25
	1.0	$2.2 \pm 0.1$	$0.691 \pm 0.007$	33.4/22	$81 \pm 43$	$7.0 \pm 1.6$	$0.51 \pm 0.07$	$32 \pm 16$	7.2/20
	0.5	$1.9 \pm 0.2$	$0.55 \pm 0.02$	5.8/11	$9 \pm 14$	$3.2 \pm 1.4$	$0.44 \pm 0.14$	$5 \pm 9$	4.6/9
900	2.4	$2.45 \pm 0.09$	$0.794 \pm 0.005$	28/34	$(2.8 \pm 1.3)10^2$	$9.4 \pm 2.3$	$0.63 \pm 0.06$	$70 \pm 31$	6.4/32
	2.0	$2.27 \pm 0.09$	$0.769 \pm 0.006$	18.7/31	$(1.7 \pm 0.9)10^2$	$7.8 \pm 2.0$	$0.62 \pm 0.07$	$47 \pm 24$	2.9/29
	1.5	$2.4 \pm 0.1$	$0.709 \pm 0.007$	23.8/26	$(1.5 \pm 0.8)10^2$	$8.6 \pm 2.4$	$0.48 \pm 0.09$	$51 \pm 25$	1.7/24
	1.0	$2.6 \pm 0.1$	$0.603 \pm 0.009$	21.6/20	$72 \pm 46$	$6.8 \pm 2.0$	$0.37 \pm 0.10$	$31 \pm 18$	2.7/18
	0.5	$2.4 \pm 0.3$	$0.44 \pm 0.02$	1.7/10	$6 \pm 16$	$2.6 \pm 1.6$	$0.36 \pm 0.17$	$4 \pm 10$	1.1/8

TABLE IV: The results of analysis of MD of the charged particle pairs in  $pp$  collisions in the limited phase-space regions  $|\eta| < \eta_c$  by the negative binomial distribution (NBD) and generalized hypergeometric distribution (GHD). The data measured by the ALICE Collaboration are taken from Ref. [13]. The NSD data sample is used in the analysis at  $\sqrt{s} = 2360$  and 900 GeV.

$\sqrt{s}$ (GeV)	$\eta_c$	NBD			GHD				
		k	q	$\chi^2/\text{NDF}$	$\alpha_0/\beta_2$	$\alpha_2/\beta_2$	$\alpha_3/\beta_2$	$\beta_0/\beta_2$	$\chi^2/\text{NDF}$
7000	1.0	$1.18 \pm 0.02$	$0.827 \pm 0.002$	116.4/37	$29 \pm 6$	$4.7 \pm 0.3$	$0.73 \pm 0.02$	$13 \pm 2$	9.8/35
2360	1.3	$1.75 \pm 0.07$	$0.782 \pm 0.006$	42.7/29	$(1.6 \pm 1.1)10^2$	$8.3 \pm 3.4$	$0.59 \pm 0.12$	$53 \pm 35$	23.4/27
	1.0	$1.67 \pm 0.08$	$0.742 \pm 0.008$	19.6/23	$44 \pm 45$	$4.9 \pm 2.2$	$0.65 \pm 0.10$	$18 \pm 18$	5.3/21
	0.5	$1.66 \pm 0.14$	$0.576 \pm 0.014$	4.9/14	$12 \pm 20$	$3.3 \pm 1.9$	$0.46 \pm 0.17$	$7 \pm 12$	3.4/12
900	1.3	$2.15 \pm 0.08$	$0.702 \pm 0.006$	29.9/25	$(2.1 \pm 1.6)10^2$	$10.2 \pm 5.1$	$0.39 \pm 0.20$	$70 \pm 54$	16.5/23
	1.0	$2.00 \pm 0.09$	$0.656 \pm 0.008$	12.3/19	$68 \pm 64$	$6.0 \pm 2.9$	$0.47 \pm 0.15$	$28 \pm 26$	6.8/17
	0.5	$2.14 \pm 0.17$	$0.458 \pm 0.014$	3.9/11	$29 \pm 37$	$4.8 \pm 3.3$	$0.15 \pm 0.32$	$19 \pm 24$	0.8/9

TABLE V: The results of analysis of MD of the charged particle pairs in  $pp$  collisions in the limited phase-space regions  $|\eta| < \eta_c$  by the negative binomial distribution (NBD) and generalized hypergeometric distribution (GHD). The data measured by the ATLAS Collaboration are from Ref. [14]. The sample with the selection  $p_T > 100$  MeV and  $n_{ch} \geq 2$  is used in the analysis.

$\sqrt{s}$ (GeV)	$\eta_c$	NBD			GHD				
		k	q	$\chi^2/\text{NDF}$	$\alpha_0/\beta_2$	$\alpha_2/\beta_2$	$\alpha_3/\beta_2$	$\beta_0/\beta_2$	$\chi^2/\text{NDF}$
7000	2.5	$1.152 \pm 0.003$	$0.9263 \pm 0.0003$	4397/54	$(2.4 \pm 0.2)10^2$	$7.3 \pm 0.3$	$0.826 \pm 0.006$	$59 \pm 4$	45.3/52
900	2.5	$2.32 \pm 0.02$	$0.790 \pm 0.002$	787/35	$(3.7 \pm 0.7)10^2$	$10.6 \pm 1.3$	$0.60 \pm 0.04$	$94 \pm 17$	29.2/33

TABLE VI: The results of analysis of MD of the charged particle pairs in  $p\bar{p}$  collisions in the limited phase-space regions  $|\eta| < \eta_c$  by the negative binomial distribution (NBD) and generalized hypergeometric distribution (GHD). The data measured by the UA5 Collaboration are taken from Ref. [24].

$\sqrt{s}$ (GeV)	$\eta_c$	NBD			GHD				
		k	q	$\chi^2/\text{NDF}$	$\alpha_0/\beta_2$	$\alpha_2/\beta_2$	$\alpha_3/\beta_2$	$\beta_0/\beta_2$	$\chi^2/\text{NDF}$
900	5.0	$4.26 \pm 0.13$	$0.799 \pm 0.006$	95.2/53	$(5.5 \pm 4.8)10^3$	$39 \pm 29$	$0.3 \pm 0.4$	$(7.7 \pm 6.5)10^2$	5.8/51
	3.0	$2.49 \pm 0.11$	$0.819 \pm 0.006$	25/42	$(7.1 \pm 5.9)10^2$	$13 \pm 7$	$0.6 \pm 0.2$	$(1.4 \pm 1.2)10^2$	5.6/40
	1.5	$2.14 \pm 0.13$	$0.725 \pm 0.012$	13.2/26	$(1.3 \pm 1.5)10^2$	$7.5 \pm 5.1$	$0.56 \pm 0.21$	$(4.4 \pm 5.0)10^1$	0.6/24
	0.5	$1.78 \pm 0.27$	$0.48 \pm 0.03$	0.7/10	$(0.2 \pm 1.3)10^{-4}$	$1.77 \pm 0.09$	$0.50 \pm 0.04$	$(1.3 \pm 9.3)10^{-5}$	0.3/8
200	5.0	$5.52 \pm 0.37$	$0.654 \pm 0.015$	7.2/29	$(2.9 \pm 0.6)10^3$	$31.5 \pm 2.5$	-	$(4.9 \pm 0.9)10^2$	0.8/28
	3.0	$4.06 \pm 0.27$	$0.663 \pm 0.015$	8.7/26	$(1.6 \pm 0.4)10^3$	$27.3 \pm 2.5$	-	$(3.5 \pm 0.7)10^2$	0.9/25
	1.5	$3.46 \pm 0.32$	$0.54 \pm 0.02$	3.4/15	$(2.8 \pm 0.9)10^2$	$13.0 \pm 1.6$	-	$(1.0 \pm 0.3)10^2$	1.7/14
	0.5	$5.5 \pm 2.1$	$0.19 \pm 0.05$	0.4/5	$13 \pm 32$	$2.4 \pm 1.3$	-	$11 \pm 25$	0.7/4

- 
- [1] Z. Koba, H. B. Nielsen, and P. Olesen, Nucl. Phys. **B40**, 317 (1972).  
[2] G. J. Alner *et al.*, (UA5 Collaboration), Phys. Lett. B **138**, 304 (1984).  
[3] V. Khachatryan *et al.*, (CMS Collaboration), J. High Energy Phys. **02**, 079 (2011).  
[4] G. J. Alner *et al.*, (UA5 Collaboration), Phys. Lett. B **160**, 199 (1985).  
[5] G. J. Alner *et al.*, (UA5 Collaboration), Phys. Lett. B **160**, 193 (1985).  
[6] K. Aamodt *et al.*, (ALICE Collaboration), Eur. Phys. J. C **68**, 68 (2010).  
[7] T. Mizoguchi and M. Biyajima, Eur. Phys. J. C **70**, 1061 (2010).  
[8] J. F. Grosse-Oetringhaus and K. Reygers, J. Phys. G **37**, 083001 (2010).  
[9] R.E. Ansorge *et al.*, (UA5 Collaboration), Z. Phys. C **43**, 357 (1989).  
[10] T. Alexopoulos *et al.*, (E735 Collaboration), Phys. Lett. B **435**, 453 (1998).  
[11] A. Giovannini and R. Ugoccioni, Phys. Rev. D **59**, 094020 (1999).  
[12] A. Giovannini and R. Ugoccioni, Phys. Rev. D **68**, 034009 (2003).  
[13] K. Aamodt *et al.*, (ALICE Collaboration), Eur. Phys. J. C **68**, 345 (2010).  
[14] G. Aad *et al.*, (ATLAS Collaboration), New J. Phys. **13**, 053033 (2011).  
[15] A. Giovannini and L. Van Hove, Z. Phys. C **30**, 391 (1986).  
[16] C. K. Chew, D. Kiang, and H. Zhou, Phys. Lett. B **186**, 411 (1987).  
[17] A. Dewanto *et al.*, Eur. Phys. J. C **57**, 515 (2008).  
[18] R. C. Hwa and C. S. Lam, Phys. Lett. B **173**, 346 (1986).  
[19] W. Feller, *An Introduction to Probability Theory and its Applications* (John Wiley & Sons, New York, 1970), Vol. I.  
[20] A. Giovannini, Nucl. Phys. **B161**, 429 (1979); P. Cvitanovic, P. Hoyer, and K. Zalevski, Nucl. Phys. **B176**, 429 (1980).  
[21] M. Biyajima and N. Suzuki, Prog. Theor. Phys. **73**, 918(1985); for a review see R. C. Hwa in *Hadronic Multiparticle production*, ed. P. Carruthers (World Scientific, Singapore, 1988).  
[22] B. Durand and I. Sarcevic, Phys. Lett. B **172**, 104 (1986); S. Sakai, Phys. Rev. D **40**, 1430 (1989).  
[23] A. V. Batunin, Mod. Phys. Lett. B **3**, 543 (1989); A. V. Batunin and O. P. Yushchenko, Mod. Phys. Lett. A **5**, 2377 (1990).  
[24] R. E. Ansorge *et al.*, (UA5 Collaboration), Z. Phys. C **43**, 357 (1989).  
[25] A. Breakstone *et al.*, (ABCDHW Collaboration), Phys. Rev. D **30**, 528 (1984).  
[26] C. Bromberg *et al.*, Phys. Rev. Lett. **31**, 1563 (1973).  
[27] A. Firestone *et al.*, Phys. Rev. D **10**, 2080 (1974).  
[28] S. Barish *et al.*, Phys. Rev. D **9**, 2689 (1974).  
[29] W. M. Morse *et al.*, Phys. Rev. D **15**, 66 (1977).  
[30] J. Whitmore, Phys. Rep. **10C**, 273 (1974).  
[31] V. V. Ammosov *et al.*, Phys. Lett. B **42**, 519 (1972).  
[32] H. Bialkowska *et al.*, Nucl. Phys. **B110**, 300 (1976).  
[33] V. Blobel *et al.*, (BHM Collaboration), Nucl. Phys. **B69**, 454 (1974).  
[34] G. Abbiendi *et al.*, (OPAL Collaboration), Eur. Phys. J. C **16**, 185 (2000).  
[35] K. Ackerstaff *et al.*, (OPAL Collaboration), Z. Phys. C **75**, 193 (1997).  
[36] G. Alexander *et al.*, (OPAL Collaboration), Z. Phys. C **72**, 191 (1996).  
[37] P. D. Acton *et al.*, (OPAL Collaboration), Z. Phys. C **53**, 539 (1992).  
[38] D. Buskulic *et al.*, (ALEPH Collaboration), Z. Phys. C **76**, 15 (1998).

- [39] P. Abreu *et al.*, (DELPHI Collaboration), Z. Phys. C **52**, 271 (1991).
- [40] H. W. Zheng *et al.*, (AMY Collaboration), Phys. Rev. D **42**, 737 (1990).
- [41] W. Braunschweig *et al.*, (TASSO Collaboration), Z. Phys. C **45**, 193 (1989).
- [42] M. Derrick *et al.*, (HRS Collaboration), Phys. Rev. D **34**, 3304 (1986).
- [43] J. L. Siegrist *et al.*, (MARK I Collaboration), Phys. Rev. D **26**, 969 (1982).